IN THE UNITED STATES PATENT AND TRADEMARK OFFICE

In re Patent Application of:
Yashwant M. Deo *et al.*

Application No.: 09/851614 Confirmation No.: 4957

Filed: May 8, 2001 Art Unit: 1644

For: HUMAN MONOCLONAL ANTIBODIES TO DENDRITIC CELLS Examiner: G. R. Ewoldt

MS Amendment
Commissioner for Patents
P.O. Box 1450
Alexandria, VA 22313-1450

DECLARATION BY DR. TIBOR KELER UNDER 37 C.F.R. §1.132

Dear Sir:

I, Dr. Tibor Keler, declare the following:

1. I am presently Vice President and Chief Scientific Officer of Celldex Therapeutics Inc. located in Phillipsburg, New Jersey, the assignee of the above-referenced patent application. I received a Ph.D. in microbiology from the University of Pennsylvania and completed a Post-Doctoral Fellowship at Fox-Chase Cancer Center in Philadelphia, Pennsylvania. My *curriculum vitae* is attached herewith as Appendix A.

2. I have reviewed claims 94-107 of the above-referenced application, drawn to an isolated human monoclonal antibody which binds to human dendritic cells comprising specific heavy and light chain CDR sequences, including conservative sequence modifications thereof.

3. I understand that claims 94-107 of the above-referenced application have been rejected as not being enabled. Specifically, the Examiner asserts that the antibodies of these claims are not enabled with respect to "conservative sequence modifications" within the CDR regions.

4. It is my opinion that, prior to the filing date of the present application, it was well within the skill of the art to have identified residues critical for binding, particularly within relatively short variable and CDR regions, and to have made conservative sequence substitutions of these residues. Moreover, the identification of critical residues would have required only routine procedures. In particular, the various methods and materials that were available, well before the filing date of the present application, are evidenced by the enclosed references (discussed in detail below). As also evidenced by these references, these methods could be used to predictably identify amino acid residues that are critical for antigen binding or are

amenable to conservative modifications. Accordingly, the prior knowledge and skill in the art, combined with the teachings contained in the present specification, would have enabled one skilled in the art to make and use the currently claimed antibodies having particular CDR sequences, as well as conservative sequence modifications thereof, without undue experimentation.

5. In particular, Brummell *et al.* ((1993) Biochem. 32:1180-1187; enclosed as Appendix B) used site-directed mutagenesis to examine the binding site of antibodies specific for *Salmonella*. Specifically, the CDR3 heavy chain domain was selected for study and a total of ninety (90) mutants were produced and screened by affinity electrophoresis / Western blots. Those of particular interest were further characterized by enzyme immunoassay and thermodynamic characterization by titration microcalorimetry. Brummell *et al.* found that antigen binding "was retained in a wide range of mutants with only one residue, Gly^{102H}, being irreplaceable."

6. Similarly, Kobayashi *et al.* ((1999) Protein Eng. 12(10):879-884), which was cited by the Examiner in the Office Action dated November 3, 2004 (and enclosed as Appendix C), states that "conservative substitution of Trp H33 by Tyr or Phe resulted in [only] moderate losses of binding affinity; however, replacement by Ala [*i.e.*, a non-conservative modification] had a significantly larger impact." (Abstract; comments in square brackets added).

7. Burks *et al.* ((1997) PNAS USA 94:412-417; enclosed as Appendix D) used PCR mutagenesis with *in vitro* transcription/translation and ELISA for the rapid generation and characterization of antibody mutants. Specifically, the authors analyzed the role and plasticity of six key contact residues in the binding pocket of a single chain Fv antibody derived from the anti-digoxin 26-10 murine antibody. A total of 114 mutant antibodies were produced. Approximately 75% of the single amino acid mutants exhibited significant binding to one or more of the digoxin analogs, even though non-conservative sequence modifications were permitted.

8. In conclusion, as shown by the foregoing representative pre-filing publications (not to mention many other publications), the knowledge and skill in the art, at the time the present application was filed, combined with the teachings contained in the present specification, would have enabled one skilled in the art to make and use the currently claimed antibodies having particular CDR sequences, as well as conservative sequence modifications thereof, without undue experimentation.

9. I have been warned that willful false statements and the like so made are punishable by fine or imprisonment, or both, under §1001 of Title 18 or the United States Code, and that such willful and false statements may jeopardize the validity of the subject application or any patent resulting therefrom, and declare that all statements made of our own knowledge are true and that all statements made on information and belief are believed to be true.

By: Tibor Keler

Tibor Keler, Ph.D.

Date: 9/28/06

Appendix A

BIOGRAPHICAL SKETCH

NAME	POSITION TITLE
Tibor Keler	Vice President and Chief Scientific Officer, Celldex Therapeutics, Inc.

EDUCATION/TRAINING

INSTITUTION AND LOCATION	DEGREE	YEAR(s)	FIELD OF STUDY
Drexel University, Philadelphia, PA	B.S.	1982	Unified Science
Drexel University, Philadelphia, PA	M.S.	1984	Biology
University of Pennsylvania, Philadelphia, PA	Ph.D.	1989	Microbiology

A. Positions and Honors

Research Training

1987-1989 Guest Researcher: National Cancer Institute, National Institutes of Health, Bethesda, MD.
1989-1992 Postdoctoral Associate: Institute for Cancer Research, Fox Chase Cancer Center, Philadelphia, PA.
1992-1993 Research Associate: Institute for Cancer Research, Fox Chase Cancer Center, Philadelphia, PA.
1993-1997 Principal Scientist, Research & Development, Medarex, Inc., Bloomsbury, NJ.
1997-1998 Assistant Director, Immunobiology: Medarex, Inc., Bloomsbury, NJ.
1998-1999 Associate Director, Immunobiology: Medarex, Inc., Annandale NJ.
1999-2001 Director, Pre-clinical Development: Medarex, Inc. Bloomsbury, NJ.
2001-2004 Senior Director, Pre-clinical Development: Medarex, Inc. Bloomsbury, NJ.
2004-2005 Vice President, Research and Development, Celldex Therapeutics, Inc. Bloomsbury, NJ
2006-present Vice President and Chief Scientific Officer, Celldex Therapeutics, Inc. Phillipsburg, NJ

Honors, Scholarships, Fellowships

1982 Graduated with second honors in Unified Science, Drexel University

Professional Societies

American Association of Immunologists
American Society for Biochemical and Molecular Biology
American Association for Cancer Research
American Society for Microbiology
International Endotoxin Society

Issued Patents

Therapeutic multispecific compounds comprised of anti-Fcα receptor antibodies; US Patent Application 20010014328.
Cells expressing anti-Fcγ Receptor binding components; US Patent Application 6682928.
Human CTLA-4 Antibodies; US Patent 6,984,720.

B. Peer-Reviewed Publications

1. Mochan E,Keler T. Plasmin degradation of cartilage proteoglycan. Biochem Biophys Acta 1984;800:312-316.
2. Keler T, Nowotny A. Metachromatic assay for the quantitative determination of bacterial endotoxins. Anal Biochem 1986;156:189-192.

Appendix A

3. Friedman H, Blanchard DK, Newton C, Klein T, Stewart W, Keler T, et al. Distinct immunomodulatory effects of endotoxin and non-toxic lipoplysaccharide derivatives in lymphoid cultures. J Biol Response Mod 1987;6:664-671.
4. Keler T, Kovats E, Nguyen V, Samu J, Solmyo B, Nowtny A. Cytotoxicity of a novel lipid like bacterial product. Biochem Biophys Res Comm 1987;149:1033-1037.
5. Samu J, Kovats E, Nguyen V, Keler T, Nowotny A, Coughlin RT Thin-layer chroamtography of endotoxins, their derivatives and contaminants. J Chromat 1988;435:167-173.
6. Nowotny A, Keler T, Pham PH, Kovats E, Aiello A, Shonekan O, et al. Isolation of a non-endotoxic anti-tumor preparation from Serratia marcescens. J Biol Response Mod 1988;7:296-308.
7. Keler T, Smith CAD, Nowotny A. Chemistry and biology of a novel lipid contaminant of some endotoxin preparations with selective cytotoxicity to transformed cells. Adv in Exper Med and Biol 1988;256:163-184.
8. Keler T, Smith CAD. Effects on growth and energy metabolism in untransformed and transformed fibroblasts by a novel cytotoxic compound. Cancer Res 1989;49:7093-7097.
9. Solmyo B, Kovats E, Keler T, Nowotny A. Column chromatography of endotoxins. J Chromatogr 1990;525:329-338.
10. Barker CS, Bear SE, Keler T, Copeland NG, Gilbert DJ, Jenkins NA, et al. Activation of the prolactin receptor gene by promoter insertion in a Moloney murine leukemia virus-induced rat thymoma. J Virol 1992;66:6763-6768.
11. Keler T, Barker C, Sorof S. Linoleic acid specifically stimulates the growth of hepatoma cell lines transfected with the target protein of a liver carcinogen. *in* "Eicosanoids and Other Bioactive Lipids in Cancer, Inflamation, and Radiation Injury" (Nigam,S., Honn, K.J., Marnett, L.J., Walden, T. eds.) Kluwer Academic Publishers, Inc., Boston, MA. pp 435-438, 1992.
12. Keler T, Barker C, Sorof S. Specific growth stimulation in hepatoma cell lines transfected with the target protein of a liver carcinogen. Proc Natl Acad Sci USA 1992;89:4830-4834.
13. Keler T, Sorof S. Growth promotion in hepatoma cells expressing liver fatty acid binding protein. J Cell Physiol 1993;157:33-40.
14. Keler T, Khan S, Sorof S. Liver fatty acid binding protein and mitogenesis in transfected hepatoma cells. in "Eicosanoids and Other Bioactive Lipids in Cancer, Inflamation, and Radiation Injury" (Honn, K.J., Marnett, L.J., Nigam,S. eds.) Kluwer Academic Publishers, Inc., Boston, MA. 1994.
15. Graziano RF, Tempest PR, White P, Keler T, Deo Y, Ghebremariam H, et al. Construction and characterization of a Humanized Anti-g-Ig Receptor Type I (FcγRI) Monoclonal Antibody. J. Immunol 1995;155:4996-5002.
16. Gorny MK, Keler T, Burda S, Williams C, Gabriel JL, Mitchell WM, et al. Functional studies of bispecific antibodies directed against HIV-1 and the Fcγ receptor type I. Antibiot Chemother 1996;48:173-183.
17. Keler T, Li H, Cloyd M, Vitale L A, Deo YM. Development of T cell lines expressing functional HIV-1 envelope glycoproteins for evaluation of immune responses in HIV infected persons. J AIDS and Human Retroviruses 1996;13:117-126.
18. Wallace PK, Keler T, Coleman K, Fisher J, Vitale L, Graziano RF, et al. Humanized mAb H22 binds the human high affinity Fc teceptor for IgG (FcγRI), blocks phagocytosis, and modulates receptor expression. J Leukocyte Biol 1997;62:469-479.

19. Keler T, Graziano RF, Mandal A, Wallace PK, Fisher J, Guyre PM, et al. Bispecific antibody-dependent cellular cytoxicity of HER2/*neu*-over-expressing tumor aells by Fcγ receptor type I-expressing effector cells. Cancer Res 1997;57:4008-4014.

20. Wallace PK, Keler T, Guyre PM, Fanger MW. Fc□RI blockade and modulation for immunotherapy. Cancer Immunol Immunotherapy 1997;45:137-141.

21. Graziano RF, Goldstein J, Sundarapandiyan K, Somasundaram C, Keler T, Deo YM. Targeting tumor cell destruction with CD64-directed bispecific fusion proteins. Cancer Immunol Immunotherapy 1997;45:124-127.

22. Deo YM, Sundarapandiyan K, Keler T, Wallace P, Graziano RF. Bispecific molecules directed to the Fc receptor for IgA (FcαRI, CD89) and tumor antigens efficiently promote cell-mediated cytotoxicity of tumor targets in whole blood. J Immunol 1997;160:1677-1686.

23. Heijnen I, Rijks L, Schiel A, Stockmeyer B, van OjiK H, Repp R, Valerius T, Keler T, et al. Combined administration of G-CSF and anti-FcγRI bispecific antibodies efficiently generates HER-2/neu-specific cytotoxic neutrophils. J Immunol 1997;159:5629-5639.

24. Russoniello C, Somasundaram C, Schlom J, Deo YM, Keler T. Characterization of a novel bispecific antibody that mediates FcγRI-dependent killing of TAG-72-expressing tumor cells. Clin Cancer Res 1998;4:2237-2243.

25. Somasundaram C, Sundarapandiyan K, Keler T, Deo YM, Graziano RF. Development of a trispecific antibody conjugate that directs two tumor-associated antigens to CD64 on myeloid effector cells. Human Antibodies 1999;9:47-54.

26. Somasundaram C, Sundarapandiyan K, Keler T, Deo YM, Graziano RF. Development of a trispecific antibody that directs two distinct tumor-associated antigens to CD64 on myeloid effector cells. Human Antibodies 1999;9(1):47-54.

27. Posey JA, Raspect R, Verma U, Deo YM, Keler T, Marshall JL, et al. A pilot trial of GM-CSF and MDX-H210 in patients with erbB-2 positive advanced malignancies. J Immunother 1999;22:371-379.

28. van Vugt MJ, Kleijmeer MJ, Keler T, Zeelenberg I, van Dijk MA, Geuze HJ, et al. The FcγRIa (CD64) ligand binding chain triggers MHC class II antigen presentation independently of its associated FcR γ-chain. Blood 1999;94(2):808-17.

29. Keler T, Wallace PK, Vitale LA, Russoniello C, Sundarapandiyan K, Graziano RF, et al. Differential effect of cytokine treatment on FcaRI and FcgRI mediated tumor cytotoxicity by monocyte derived macrophages. J Immunol 2000;164(11):5746-52.

30. Keler T, Guyre PM, Vitale LA, Sundarapandiyan K, van de Winkel JGJ, Deo YM, et al. Targeting weak antigens to CD64 elicits potent humoral responses in human CD64 transgenic mice. J Immunol 2000;165(12):6738-42.

31. Wiener E, Mawas F, Coates P, Hossain AK, Perry M, Snachall S, Deb P, Rodeck CH, Keler T. HPA-1a-mediated platelet interaction with monocytes in vitro: involvement of Fcγ receptor (FcγR) classes and inhibition by humanised monoclonal anti-FcγRI H22. Eur J Haematol 2000;65:399-406.

32. Sundarapandiyan K, Keler T, Behnke D, Engert A, Barth S, Matthey B, et al. Bispecific antibody-mediated destruction of Hodgkin's lymphoma cells. J Immunol Methods 2001;248:113-23.

33. Guyre CA, Keler T, Swink SL, Vitale LA, Graziano RF, Fanger MW. Receptor modulation by Fc gamma RI-specific fusion proteins is dependent on receptor number and modified by IgG. J Immunol 2001;167:6303-11.

34. Wallace PK, Kaufman PA, Lewis LD, Keler T, Givan AL, Fisher JL, et al. Bispecific antibody-targeted phagocytosis of HER-2/neu expressing tumor cells by myeloid cells activated in vivo. J Immunol Methods 2001;248:167-82.

35. Wiener E, Abeyakoon O, Benchetrit G, Lyall M, Keler T, Rodeck CH. Anti-HPA-1a-mediated platelet phagocytosis by monocytes in vitro and its inhibition by Fc gamma receptor (FcgammaR) reactive reagents. Eur J Haematol. 2003 Feb;70(2):67-74.

36. Borchmann P, Treml JF, Hansen H, Gottstein C, Schnell R, Staak O, Zhang HF, Davis T, Keler T, Diehl V, Graziano RF, Engert A. The human anti-CD30 antibody 5F11 shows in vitro and in vivo activity against malignant lymphoma. Blood. 2003 Nov 15;102(10):3737-42.

37. Keler T, Halk E, Vitale L, O'Neill T, Blanset D, Lee S, Srinivasan M, Graziano RF, Davis T, Lonberg N, Korman A. Activity and safety of CTLA-4 blockade combined with vaccines in cynomolgus macaques. J Immunol. 2003; 171:6251-9

38. Ramakrishna V, Treml JF, Vitale L, Connolly JE, O'Neill T, Smith P, Jones CL, He L, Goldstein J, Wallace PK, Keler T, and Endres MJ. Mannose receptor targeting of tumor antigen pmel17 to human dendritic cells directs anti-melanoma T cell responses via multiple HLA molecules. J Immunol. 2004 Mar 1;172(5):2845-52.

39. He L, Ramakrishna V, Connolly JE, Wang XT, Smith PA, Jones CL, Valkova-Vachnova M, Arunakumari A, Treml JF, Goldstein J, Wallace PK, Keler T and Endres MJ. A novel human cancer vaccine elicits cellular responses to the tumor-associated antigen, human chorionic gonadotropin beta. Clinical Cancer Research 2004 March 15; 10 (6).

40. Keler, T.; Ramakrishna, V.; Fanger, M. W. Mannose receptor-targeted vaccines. Expert Opin Biol Ther. 2004, 4: 1953-62.

41. van Royen-Kerkhof A, Sanders EA, Wijngaarden S, van Roon JA, Voorhorst-Ogink M, Walraven V, Gerritsen A, van Dijk MA, Kuis W, Rijkers GT, Keler T, Leusen JH, van de Winkel JG.Flow cytometric determination of FcgammaRIIa (CD32) polymorphism. J Immunol Methods. 2004 Nov;294(1-2):135-44. Epub 2004 Oct 06.

42. Sanderson K, Scotland R, Lee P, Liu D, Groshen S, Snively J, Sian S, Nichol G, Davis T, Keler T, Yellin M, Weber J. Autoimmunity in a Phase I Trial of a Fully Human Anti-Cytotoxic T-Lymphocyte Antigen-4 Monoclonal Antibody With Multiple Melanoma Peptides and Montanide ISA 51 for Patients With Resected Stages III and IV Melanoma. J Clin Oncol. 2005 Feb 1;23(4):741-50.

43. van Royen-Kerkhof A, Sanders EA, Walraven V, Voorhorst-Ogink M, Saeland E, Teeling JL, Gerritsen A, van Dijk MA, Kuis W, Rijkers GT, Vitale L, Keler T, McKenzie SE, Leusen JH, van de Winkel JG. A novel human CD32 mAb blocks experimental immune haemolytic anaemia in FcgammaRIIA transgenic mice. Br J Haematol. 2005 Jul;130(1):130-7.

44. Korman A, Yellin M, Keler T. Tumor immunotherapy: preclinical and clinical activity of anti-CTLA4 antibodies. Curr Opin Investig Drugs. 2005 Jun;6(6):582-91.

45. Keler T, He L, Graziano RF. Development of antibody-targeted vaccines. Curr Opin Mol Ther. 2005 Apr;7(2):157-63.

46. Bevaart L, Goldstein J, Vitale L, Russoniello C, Treml J, Zhang J, Graziano RF, Leusen JH, van de Winkel JG, Keler T. Direct targeting of genetically modified tumour cells to Fc gammaRI triggers potent tumour cytotoxicity. Br J Haematol. 2006 Feb;132(3):317-25.

Probing the Combining Site of an Anti-Carbohydrate Antibody by Saturation–Mutagenesis: Role of the Heavy-Chain CDR3 Residues

David A. Brummell,[‡] Vidhya P. Sharma, Naveen N. Anand,[§] Doris Bilous, Ginette Dubuc, Joseph Michniewicz, C. Roger MacKenzie, Joanna Sadowska, Bent W. Sigurskjold,[∥] Barbara Sinnott, N. Martin Young, David R. Bundle, and Saran A. Narang*

Institute for Biological Sciences, National Research Council of Canada, Ottawa, Ontario K1A 0R6, Canada

Received July 17, 1992; Revised Manuscript Received October 7, 1992

ABSTRACT: The carbohydrate-binding site in Fab fragments of an antibody specific for *Salmonella* serogroup B O-polysaccharide has been probed by site-directed mutagenesis using an *Escherichia coli* expression system. Of the six hypervariable loops, the CDR3 of the heavy chain was selected for exhaustive study because of its significant contribution to binding-site topography. A total of 90 mutants were produced and screened by an affinity electrophoresis/Western blotting method. Those of particular interest were further characterized by enzyme immunoassay, and on this basis seven of the mutant Fabs were selected for thermodynamic characterization by titration microcalorimetry. With regard to residues that hydrogen bond to ligand through backbone interactions, Gly^{102H} could not be substituted, while several side chains could be introduced at Gly^{100H} and Tyr^{103H} with relatively little effect on antigen binding. There was, however, a preference for nonpolar side chains at position 103H. Substitution of His^{101H} with carboxylate and amide side chains gave mutants with binding affinities approaching that of the wild type; complete side-chain removal by mutation to Gly was tolerated with a 10-fold reduction in binding constant. Analysis of binding by titration microcalorimetry revealed some dramatic thermodynamic changes hidden by the similarity of the binding constants. Similar effects were observed with residue changes in an Arg-Asp salt-bridge at the base of the loop. These results indicate that alterations to higher affinity anti-carbohydrate antibodies are characterized by an enthalpy–entropy compensation factor which allows for fundamental changes in the nature of the binding interactions but impedes engineering for increases in affinity.

As evidence for the crucial role of carbohydrates as recognition elements in cellular functions increases, so does the desirability of gaining a full understanding of how the biological roles of carbohydrates are exerted through their interactions with proteins (Vyas, 1991). A recent increase in the number of well-refined structures has provided considerable insight into the atomic interactions at play in these processes. In our laboratory, the details of carbohydrate binding by antibodies have, for the first time, been described at atomic resolution. The crystal structure of a Fab complexed with a *Salmonella* O-antigen of serogroup B has been solved at 2.05-Å resolution (Cygler et al., 1991). The antigen, built from the four-sugar repeating unit

$$\rightarrow 2)[\alpha\text{D-Abe}^{1}(1\rightarrow 3)]\alpha\text{D-Man}(1\rightarrow 4)\alpha\text{L-Rha}(1\rightarrow 3)\alpha\text{D-Gal}(1\rightarrow$$

is bound in a "pocket"-like site via a network of hydrogen bonds and van der Waals contacts (Figure 1). Abequose, the immunodominant sugar, is totally buried, while mannose and galactose residues lie on the protein surface and are partially exposed to water.

We have initiated a protein engineering study of the combining site of the anti-*Salmonella* antibody to test the various site residues and to complement antigen analog studies. Such detailed analyses of well-defined protein–carbohydrate structures are necessary to understand the principles governing the relationship among structure, specificity, and affinity in carbohydrate recognition systems. Without this type of information, strategic and astute redesign of carbohydrate binding sites will be difficult. Structure–function studies by site-directed mutagenesis have to date been confined to sugar-binding proteins from the bacterial periplasm (Quiocho, 1991; Vermersch et al., 1990, 1991). As a model system for this type of study, the *Salmonella* antibody offers several advantages in addition to the well-refined crystal structure. These include a detailed description of binding thermodynamics (Sigurskjold et al., 1991; Sigurskjold & Bundle, 1992) and an efficient *Escherichia coli* expression system (Anand et al., 1990, 1991a) that yields active product through the use of bacterial signal peptides (Better et al., 1988; Skerra & Plückthun, 1988). With a binding constant of 2×10^5 M^{-1}, the anti-*Salmonella* antibody has very good affinity for an anti-carbohydrate antibody.

Antibody binding sites are constructed chiefly from six segments, three from each chain, termed CDRs. The origin of the CDR-H3 from the D-segment of the gene together with junctional and N-diversity (Alt & Baltimore, 1982) leads to far greater sequence variation in this CDR than in the other five. As often occurs in antibodies (Alzari et al., 1988; Mian et al., 1991), the heavy-chain CDR3 of the *Salmonella* antibody makes a greater contribution to antigen binding than do the other five CDR loops. Four of the eight residues that form hydrogen bonds to the antigen reside in this loop (Figures 1 and 2). Another feature of the H3 loop is the presence at

* Author to whom correspondence should be addressed [telephone (613) 990-3247; fax (613) 941-1327].

‡ Present address: Department of Vegetable Crops, Mann Laboratory, University of California, Davis, CA 95616-8631.

§ Present address: Connaught Laboratories Ltd., Willowdale, ON, Canada.

∥ Present address: Department of Chemistry, Carlsberg Laboratory, DK-2500 Copenhagen Valby, Denmark.

⊥ Abbreviations: Abe, 3,6-dideoxy-*xylo*-hexose; BSA, bovine serum albumin; CDR, complementary-determining region; ETA, enzyme immunoassay; H3, heavy-chain CDR3; PVDF, poly(vinylidene fluoride).

0006-2960/93/0432-1180$04.00/0 Published 1993 by the American Chemical Society

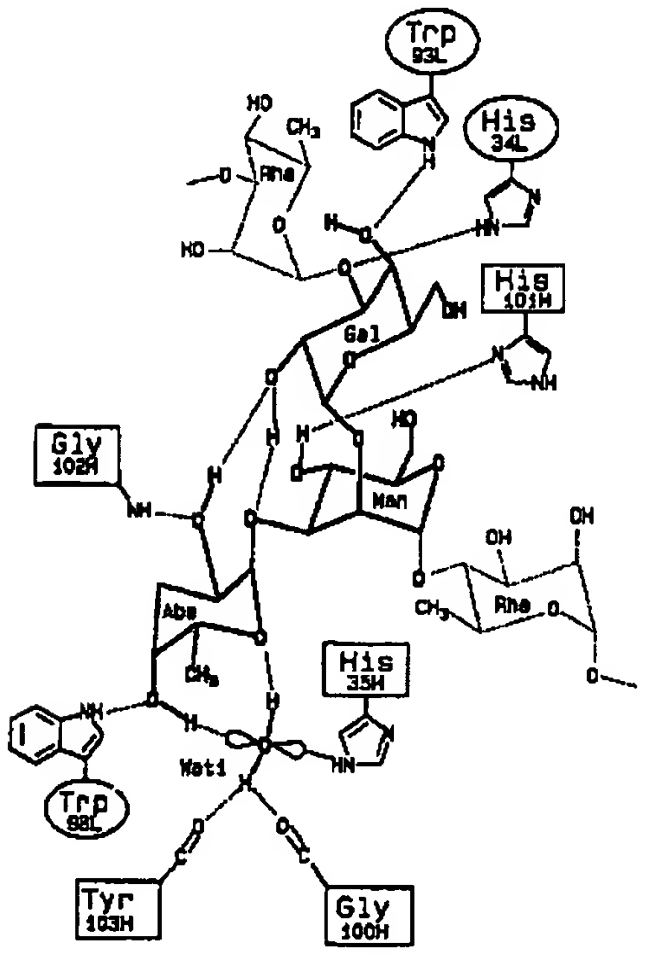

FIGURE 1: Details of Se155-4 CDR-H3 involvement in binding the trisaccharide epitope of *Salmonella* serogroup B O-antigen: hydrogen-bonding scheme highlighting H3 residue (in boxes) involvement.

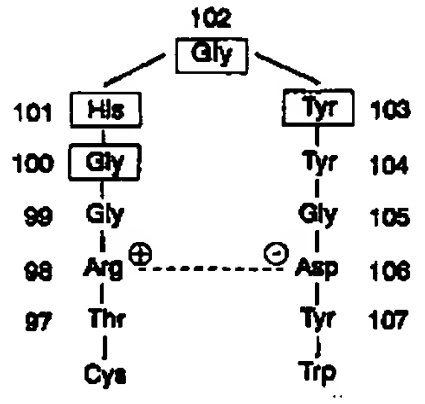

FIGURE 2: Heavy-chain CDR3 sequence indicating the residues (in boxes) which hydrogen-bond to antigen and the position of the Arg^{94H}–Asp^{106H} salt-bridge.

its base of a salt-bridge (Chothia & Lesk, 1987) which may stabilize its conformation (Figure 2). In other antibodies alterations to this salt-bridge gave unpredictable and interesting results (Chien et al., 1989; Novotny et al., 1990; Panka et al., 1988). For these reasons, our combining site engineering studies have focused on H3. In this paper we describe the results of mutagenesis of each of the four H3 contact residues into each of the other 19 amino acid side chains. Such a systematic approach may lead to a better appreciation of the role of this key CDR in the formation of the antigen binding site.

EXPERIMENTAL PROCEDURES

Materials. Restriction enzymes and DNA-modifying enzymes were purchased from New England Biolabs and Bethesda Research Laboratories. All DNA manipulations were carried out essentially as described by Sambrook et al. (1989). Oligonucleotides were synthesized on an Applied Biosystems Model 380A automatic DNA synthesizer. Enzyme conjugates and substrates for immunoassays were obtained from Caltag, Kirkegaard and Perry Laboratories and Bio-Rad.

Fab Gene Construction. The dicistronic Fab construct pSal–Fab (Anand et al., 1991a) consisting of the Fd and light chain genes, each preceded by the *ompA* signal peptide, in the expression plasmid pUCE8 (Narang et al., 1987) was modified somewhat prior to the initiation of this study. An unpaired cysteine (Cys^{94L}) was mutated to Ser, using the codon TCT, to eliminate unwanted disulfide bond formation. This change had no detectable effect on antigen binding as measured by enzyme immunoassay (data not shown). Also, a single base pair error at heavy-chain residue 65 (AGT, encoding Ser, instead of the required CGT, encoding Arg) was corrected. This was accomplished by replacing the *Pfl*MI (Thr^{30H}) to *Spe*I (Thr^{74H}) segment with six synthetic oligonucleotides, at the same time changing the GAG Glu^{46H} codon to GAA, thus destroying the *Xho*I site at Leu^{45H}, and changing the CGT Arg^{40H} codon to CGG, thereby generating an *Eag*I site. The corrected plasmid was designated pSal–FabB. The pSal–FabB product had an affinity for antigen that was approximately 50% better than that of the Ser^{65H} mutant (pSal–Fab product).

Generation of Mutants. Site-directed mutagenesis was carried out by a double-mutation approach (Narang et al., 1991). For heavy-chain substitutions between positions 100H and 106H, pSal–FabB was cut at the unique *Mlu*I (at Thr^{97H}) and *Sac*I (at Ser^{117H}) sites and the *Mlu*I–*Sac*I segment was replaced in each cloning with four synthetic oligonucleotides (Figure 3). In each instance, the left-hand pair of oligonucleotides possessed one to three mismatches which introduced the codon for one substitution on the top strand and the anticodon for the second substitution on the bottom strand. The right-hand pair of oligonucleotides was common for each cloning and possessed a single silent mismatch at position 112H, with the result that clones derived from the top strand gained an extra *Kas*I site and clones derived from the bottom strand gained an extra *Nhe*I site. These restriction sites were used to screen miniprep DNA prior to sequencing. A similar procedure was employed to generate mutants in the 97H–99H and 106H–107H regions, except that a unique *Bsg*I site (recognition sequence at 95H, cut site a 90H) was used instead of *Mlu*I and the junction between the two pairs of oligonucleotides was moved five amino acids to the left. In all cases nucleotide sequences were confirmed by sequencing with the dideoxy method using the Sequenase kit (U.S. Biochemicals Corp.).

Expression and Isolation of Mutant Fabs. E. coli, strain TG-1, harboring wild-type or mutant pSal–FabB plasmid was grown with shaking at 30 °C in M9 medium supplemented with 0.4% (w/v) casamino acids and 5 mg/L thiamin, in the presence of 100 mg/L ampicillin. At 24 h, cultures were induced by adding supplementary nutrients (12 g of tryptone, 24 g of yeast extract, and 4 mL of glycerol per liter) and 1 mM isopropyl thiogalactopyranoside. After a further 66 h of growth, active Fab was isolated from periplasmic extracts by affinity chromatography as described previously (Anand et al., 1991a).

Affinity Electrophoresis. An affinity electrophoresis method using acrylamide gels containing antigen was developed on the basis of principles originally described by Takeo and coworkers (Takeo & Nakamura, 1972; Takeo & Kabat, 1978). Native polyacrylamide gels were made for the PhastSystem (Pharmacia). Separating gels were 8% acrylamide in 112 mM Tris acetate buffer, pH 6.4, and stacking gels were 3% acrylamide in 56 mM Tris acetate buffer, pH 6.4. For ligand-

A. WILD-TYPE SEQUENCE OF MUTAGENESIS CASSETTE

```
                  CDR3
         ___________________________
 97  98  99 100 101 102 103 104 105 106 107 108 109 110 111 112 113 114 115 116 117 118
Thr Arg Gly Gly His Gly Tyr Tyr Gly Asp Tyr Trp Gly Gln Gly Ala Ser Leu Thr Val Ser Ser

CG CGT GGT GGT CAT GGT TAC TAC GGT GAT TAC TGG GGT CAG GGC GCC AGC CTG ACC GTG AGC T
    A CCA CCA GTA CCA ATG ATG CCA CTA ATG ACC CCA GTC CCG CGG TCG GAC TGG CAC

 MluI                                                                       SacI
```

B. LEFT-HAND REPLACEMENT OLIGONUCLEOTIDES

```
 97  98  99 100 101 102 103 104 105 106
Thr Arg Gly Gly His Arg Tyr Tyr Gly Asp

CG CGT GGT GGT CAT CGT TAC TAC GGT GAT
    A CCA CCA GTA TTT ATG ATG CCA CTA ATG ACC

 MluI             anti-
                   Lys
```

C. RIGHT-HAND REPLACEMENT OLIGONUCLEOTIDES

```
107 108 109 110 111 112 113 114 115 116 117 118
Tyr Trp Gly Gln Gly Ala Ser Leu Thr Val Ser Ser

                 KasI
TAC TGG GGT CAG GGC GCC AGC CTG ACC GTG AGC T
        CCA GTC CCG CGA TCG GAC TGG CAC

                 NheI         SacI
```

FIGURE 3: Cloning procedure for the generation of CDR-H3 mutants. The wild-type sequence (A) was replaced by four oligonucleotides: two left-hand oligos (B) encoding the desired mutations and two right-hand oligos (C) that introduced a *Kas*I site in clones derived from the top strand and an *Nhe*I site in clones derived from the bottom strand. The same right-hand oligos were used in all clonings. In this example, position 102H is changed to arginine (and gains a *Kas*I restriction site) or lysine (and gains an *Nhe*I restriction site). Mismatches are double-underlined.

containing gels, *Salmonella* serogroup B O-antigen prepared from *Salmonella essen* lipopolysaccharide (Svenson & Lindberg, 1978) was added to separating gel mixtures to 0.005% (w/v) prior to polymerization. This antigen concentration would give at least at 50-fold excess of antigen over antibody in gels, assuming a Fab production level of 20 mg/L of bacterial culture, and meets the requirements described by Takeo and Kabat (1978). Native buffer strips were obtained from Pharmacia. Fab samples were electrophoresed in gels with and without antigen at 10 mA for 268 Vh as recommended by Pharmacia for native gels. Following electrophoresis, Western blots were made simply by placing the gel in contact with PVDF membrane (Millipore) that had been wetted in methanol and soaked in 25 mM Tris–192 mM glycine, pH 8.4. The contact time was 2 min with three consecutive blots being taken from the same gel. The blots were developed with an anti-mouse lambda-chain–alkaline phosphatase conjugate (Caltag). The second and third blots from each gel generally gave less background staining. The distances to which Fab bands migrated in the presence and absence of antigen were measured from the blots. The degree to which wild-type Fab migration was retarded by antigen

$$(d - d_{Ag})/d$$

where d is the distance migrated in the absence of antigen and d_{Ag} the distance in the presence of antigen, was assigned a value of 1, and values for mutant Fab retardation relative to that of the wild-type were calculated.

Binding Assays. Following preliminary screening by affinity electrophoresis, the antigen-binding properties of mutants of particular relevance were further investigated by indirect EIA. These assays were carried out as described previously (Anand et al., 1991b) using microtiter plates coated with BSA–O-polysaccharide conjugate (E. Altman, unpublished results).

The binding thermodynamics of selected mutants were determined by titration microcalorimetry using an OMEGA titration microcalorimeter (Wiseman et al., 1989) from Microcal Inc. (Northampton, MA). Wild-type and mutant Fabs, at concentrations of approximately 50 μM in 50 mM Tris and 150 mM NaCl, pH 8.0, were titrated with a 2 mM solution of synthetic trisaccharide antigen in the same buffer at 25 °C. The ligand solution was injected in 20 portions of 5 μL. Thermogram data were analyzed as described previously (Sigurskjold et al., 1991; Sigurskjold & Bundle, 1992).

RESULTS

Targeting H3 Mutations. The H3 loop of Se155-4 consists of nine residues (99H–107H, sequential numbering system). Four of these residues, all from the D-region, form hydrogen bonds with the bound trisaccharide (Figures 1 and 2). The loop is also characterized by a salt-bridge, at its base, between Arg^{98H} and Asp^{106H}. The loop is quite short compared to H3 loops in general and is characterized by a predominance of glycine and tyrosine residues, with Gly^{100H}, Gly^{102H}, and Tyr^{103H} forming hydrogen bonds to antigen and to a structured water molecule through NH and C=O groups of the main chain. Tyr^{103H} also contributes one of several aromatic side chains that define the binding site. His^{101H} accepts a hydrogen bond from O-4 of mannose and is one of three histidine residues participating in the hydrogen-bond network. Although His^{101H} is largely exposed to solvent (Figure 4), antigen mapping studies have shown that its interaction with mannose is important. These four D-region contact residues were targeted for site-directed mutagenesis because of their role in antigen binding and the fact that they are representative of the types of interactions that characterize carbohydrate binding by Se155-4. The role of the Arg^{98H}–Asp^{106H} salt-bridge in maintaining the integrity of the combining site was also probed

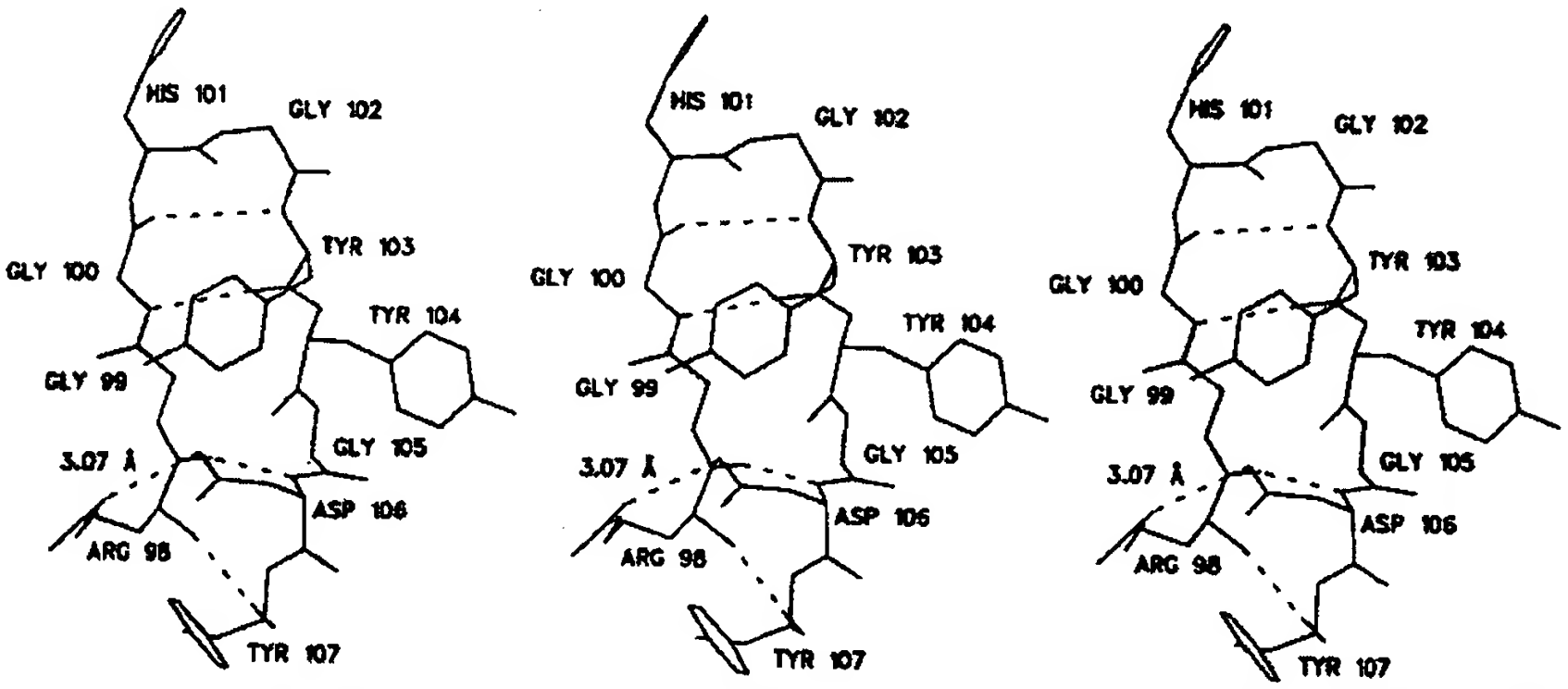

FIGURE 4: Stereoview of the wild-type heavy-chain CDR3 loop showing internal hydrogen bonds and the position of the Arg^{98H}–Asp^{106H} salt-bridge.

Table I: Affinity Electrophoresis Analysis of Antigen-Binding Activity of H3 Contact Residue Mutants[a]

changed to	Gly^{100H}	His^{101H}	Gly^{102H}	Tyr^{103H}
Ala	0.9	0.55	0.75	ND[b]
Arg	0.85	0.35	0.05	ND
Asn	0.9	0.9[c]	0.1	0.75
Asp	0.9	1.0[c]	0	0.5
Cys	ND	ND	ND	ND
Glu	1.0	0.85[c]	0.05	0.8
Gln	0.9	0.9[c]	0.1	0.8
Gly	1.0	0.85[c]	1.0	0.75
His	0.9	1.0	0.15	0.9
Ile	0.35	0.45	0.2	0.9
Leu	0.7	0.4	0.15	0.95
Lys	0.9	0.5	0.05	ND
Met	0.8	0.5	0.25	0.85
Phe	0.85	0.3	0.1	0.9
Pro	0.4	0.8	0.05	0.2
Ser	0.9	0.75	0.45	0.7
Thr	0.65	0.5	0.35	0.8
Trp	0.95	0.1	ND	0.9
Tyr	0.9	0.4	0.1	1.0
Val	0.05	0.55	0.05	0.9

[a] The values of relative retardation are given to ±0.05. [b] Fab band not detected. [c] Microcalorimetry also done.

by a limited number of amino acid substitutions. Both salt-bridge residues are partially buried and quite distant from the binding site (Figure 4).

Expression and Mutagenesis of Se155-4 Fab. Active Fab fragments with interchain disulfide bonds formed in good yield in the *E. coli* periplasm. The double-replacement mutagenesis technique provided an efficient means of mutant generation. Mutants identified by preliminary restriction-cut screening were confirmed to have the correct sequence 8 of 10 times. The wild-type construct gave 3–5 mg/L of active periplasmic product, but the yields of mutant Fabs were sometimes dramatically higher or lower. The five His^{101H} substitutions that gave the most active Fab molecules (Table I) had yields of 15–20 mg/L. In contrast, Western blotting indicated that introduction of cysteine residues into the loop resulted in poor yields of secreted product. Western blotting and Coomassie staining of affinity chromatography fractions showed that, for active mutants, all of the periplasmic Fab was fully active.

Affinity Electrophoresis. Mutant Fabs were screened for antigen-binding activity by an affinity electrophoresis/Western

FIGURE 5: Affinity electrophoresis of wild-type and mutant Fabs. Western blots were prepared following the electrophoresis of identical samples in the absence (A) and presence (B) of *Salmonella* serogroup B O-antigen in the gel. The top of the separating gel is at the top of the photograph, and a free light-chain band is visible at the bottom of the gel in lane 3. 1, Wild-type; 2, $His^{101H}Asp$; 3, $His^{101H}Phe$; 4, $Asp^{104H}Tyr$-$Tyr^{107H}Asp$.

blotting technique developed specifically for this purpose. The procedure has the double advantage of screening simultaneously for periplasmic Fab presence and activity. In instances involving a change in molecular charge, the mutation is also confirmed by a mobility change in the native gels (Figure 5). The detection sensitivity was such that unconcentrated periplasmic extracts generally gave strong Fab bands using the standard assay conditions. As a screening method, the technique is considerably more accurate than previously used column procedures (Narang et al., 1991).

CDR Mutants. The 4 H3 residues that hydrogen bond to the oligosaccharide were mutated to all other 19 amino acids. Wild-type Fab controls were included as a check on techniques (Table I). Fab bands were readily detectable, by affinity electrophoresis, in periplasmic extracts of most mutants with

Table II: Relative Affinity for Antigen of Salt-Bridge Mutants As Estimated by Retardation during Affinity Electrophoresis[a]

	mutation[a]					retardation relative to wild type
	Thr^{97H}	Arg^{98H}	Gly^{99H}	Asp^{106H}	Tyr^{107H}	
1	–	Ala	–	–	–	0.2
2	–	–	–	Ala	–	0.85
3	–	–	–	Asn	–	0.9
4	–	Lys	–	–	–	1.0
5	–	–	–	Glu	–	0.95
6	–	Lys	–	Glu	–	1.0
7	–	Asp	–	Arg	–	0.3
8	–	–	–	Tyr	Asp	1.05
9	–	–	–	Tyr	Glu	ND[b]
10	–	Lys	–	Tyr	Asp	0.9
11	–	Lys	–	Tyr	Glu	0.95
12	Arg	Thr	–	–	–	0
13	–	Gly	Arg	–	–	ND

[a] Dashes denote wild-type amino acid. [b] Fab band not detected.

the notable exception of those involving the incorporation of a cysteine residue into the loop. The results indicated that none of the mutations resulted in improved affinity.

The affinity electrophoresis results showed that Gly^{100H}, which accepts a H-bond from the ordered water molecule, could be replaced by several amino acids without drastic loss of binding activity. On the basis of titration microcalorimetry data indicating that an affinity electrophoresis value of 0.85 represented a 10-fold drop in binding constant, approximately 60% of the mutants had affinities that were within an order of magnitude of that of the wild type. Surprisingly, very large side chains could be introduced without much effect; the activity of Gly^{100H}Trp, for example, resembled that of the wild type. On the other hand, any substitution of Gly^{102H} resulted in an enormous drop in activity. Results for the Tyr^{103H} position, at which the backbone C═O group accepts a H-bond from the ordered water molecule, indicated a preference for an alkyl/hydrophobic side chain, with such residues giving binding affinities within an order of magnitude of that of the wild type.

A more exhaustive study of the His^{101H} changes was undertaken to probe the histidine–sugar interactions that are so prominent in antigen binding by Se155-4. Introduction of hydrophobic side chains at this position virtually abolished binding. The best substitutions were aspartic acid, asparagine, glutamic acid, and glutamine. However, side-chain removal, i.e., His^{101H}Gly, was also tolerated to a remarkable degree. His^{101H}Pro and His^{101H}Ser were also moderately active. The five most active mutants as screened by affinity electrophoresis were selected for more in-depth analysis and were purified by affinity chromatography. Indirect EIA performed with the purified Fabs confirmed the affinity electrophoresis results, giving an activity ranking of His > Asp > Asn > Gln > Glu > Gly (data not shown).

Salt-Bridge Alterations. The construction of the various salt-bridge mutants and the affinity electrophoresis data obtained for them are presented in Table II. The results confirmed the requirement of a positively charged residue at position 98H and to a lesser degree the importance of a negatively charged residue at position 106H. While Arg^{98H}-Lys was fully active, Arg^{98H}Ala exhibited a complete loss of binding activity. The absolute requirement for positive charge at position 98H was further confirmed by the Thr^{97H}Arg and Arg^{98H}Thr double mutation. Glutamic acid was a good replacement for Asp at position 106H, but the requirement for a negative charge at this position was considerably less stringent since both Asp^{106H}Ala and Asp^{106H}Asn displayed relatively good activity. Of particular interest was the double mutant Asp^{106H}Tyr and Tyr^{107H}Asp, which displayed binding activity that was higher than that of the wild type. This was observed by affinity electrophoresis (Table II) and confirmed by indirect EIA, with the latter method indicating a 3-fold increase in activity (data not shown).

Titration Microcalorimetry. A thermodynamic analysis of the five most active His^{101H} mutants and the most active salt-bridge mutant was obtained by titration microcalorimetry (Table III). The results confirmed the reliability of the affinity electrophoresis technique as a screening procedure insofar as all five had K_a values of $\geq 2 \times 10^4\ M^{-1}$. At the His^{101H} position, an increase of over 50% in the enthalpy terms was observed for the Glu and Gln mutants. However, an opposing entropic effect precluded any increase in affinity. Affinities, in fact, were 3–4 times less than that of the wild type. This dramatic shift in thermodynamic parameters was not observed for the Asp and Asn mutants. With these mutants, ΔH° values were somewhat lower and ΔS° values relatively unchanged relative to those of the wild type. This indicated that these structural changes have little effect on binding chacteristics other than slightly weaker hydrogen bonding or van der Waals forces. The complete removal of the 101H side chain in the glycine mutant gives a molecule displaying a 10-fold lower affinity [$(2 \pm 0.5) \times 10^4\ M^{-1}$], a highly favorable enthalpy term and a highly unfavorable entropy term. Such a result is open to several interpretations, such as water-mediated hydrogen bonding or improved contacts provided by a more flexible H3 loop. The calorimetric data for the salt-bridge mutant in which the positions of Asp^{106H} and Tyr^{107H} were reversed indicated that binding by the double mutant was completely enthalpy driven with neither positive nor negative contribution from the entropy term. However, unlike the electrophoresis and indirect EIA results which indicated higher activity for the double mutant, the binding constant of the double mutant as determined by microcalorimetry [$(1.7 \pm 0.3) \times 10^5\ M^{-1}$] was the same as that of the wild type. Changing the salt-bridge partners to Lys and Glu resulted in a higher enthalpy term that was offset by an unfavorable entropy change.

DISCUSSION

Proteins that recognize carbohydrates must meet the unique challenge of discriminating among a vast number of sugar structures arising from the stereochemistry of hydroxyl groups in monosaccharides and different sugar linkage possibilities. Failure in this regard could be disastrous since carbohydrates are used as the recognition molecules in key cellular processes (Feizi, 1991). With a number of well-refined crystal structures of protein–carbohydrate complexes now solved (Quiocho, 1991; Vyas, 1991), some insight into how these strict requirements are met is being acquired. The atomic features of carbohydrate binding are best understood for the bacterial periplasmic receptors involved in sugar transport (Quiocho, 1991). With dissociation constants in the micromolar range, these proteins are at the upper end of the affinity spectrum for sugar-binding proteins. They are characterized by binding sites that are largely buried and solvent inaccessible, a stacking of aromatic residues against the sugar ring, and hydrogen bonding of sugar hydroxyls to polar amino acid side chains (Quiocho, 1991; Spurlino et al., 1991; Vyas et al., 1991). A considerable amount of information is also available on sugar binding by plant lectins and anti-carbohydrate antibodies (Bundle & Young, 1992). These proteins, characterized by affinities that are somewhat lower than those of the periplasmic receptors, have binding sites that are near the protein surface

Table III: Thermodynamic Parameters for Antigen Binding by Selected H3 Mutants of Se155-4

	K (M^{-1})	$\Delta G°$ (kJ mol^{-1})	$\Delta H°$ (kJ mol^{-1})	$-T\Delta S°$ (kJ mol^{-1})
E. coli WT Fab	$(2.1 \pm 0.3) \times 10^5$	-30.3 ± 0.4	-24.8 ± 0.6	-5.5 ± 0.7
$His^{101H} \rightarrow Glu$	$(3.7 \pm 1.0) \times 10^4$	-26.1 ± 0.7	-44.4 ± 5.5	18.3 ± 5.5
$His^{101H} \rightarrow Gln$	$(7.6 \pm 2.1) \times 10^4$	-27.9 ± 0.7	-36.1 ± 3.0	8.2 ± 3.1
$His^{101H} \rightarrow Asp$	$(7.1 \pm 1.5) \times 10^4$	-27.7 ± 0.5	-22.3 ± 1.2	-5.3 ± 1.3
$His^{101H} \rightarrow Asn$	$(6.0 \pm 1.2) \times 10^4$	-27.2 ± 0.5	-23.1 ± 1.3	-4.2 ± 1.4
$His^{101H} \rightarrow Gly$	$(2.0 \pm 0.5) \times 10^4$	-24.6 ± 0.6	-41.1 ± 5.5	16.6 ± 5.5
$Arg^{98H} \rightarrow Lys$ and $Asp^{106H} \rightarrow Glu$	$(5.8 \pm 1.0) \times 10^4$	-27.2 ± 0.4	-39.3 ± 2.0	12.1 ± 2.1
$Asp^{106H} \rightarrow Tyr$ and $Tyr^{107H} \rightarrow Asp$	$(1.7 \pm 0.3) \times 10^5$	-30.0 ± 0.4	-29.2 ± 1.0	-0.7 ± 1.1

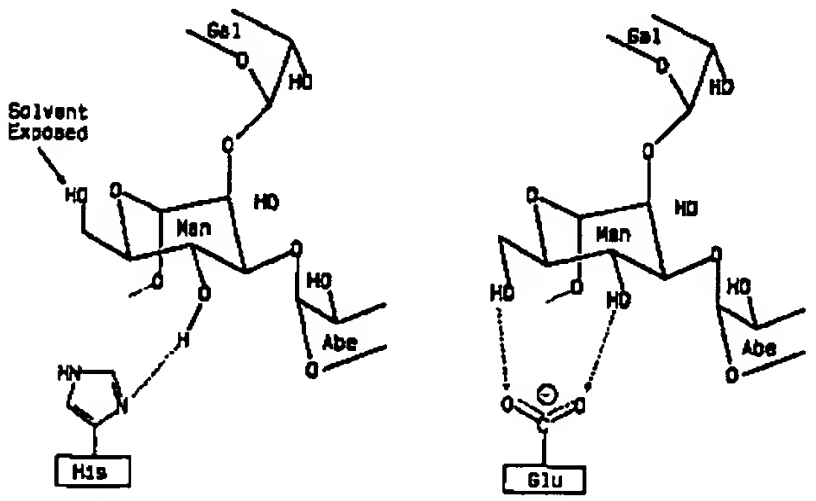

FIGURE 6: Postulated hydrogen-bond changes associated with His^{101H}-Glu mutation. The hydrogen-bonding scheme for O-4 of the mannose residue is shown for the native complex and for the His^{101H}Glu mutant. Although Glu is shown here, this potential bidentate hydrogen bonding to mannose O-4 and O-6 could be achieved with Asp, Asn, and Gln and might require the participation of a bound water molecule.

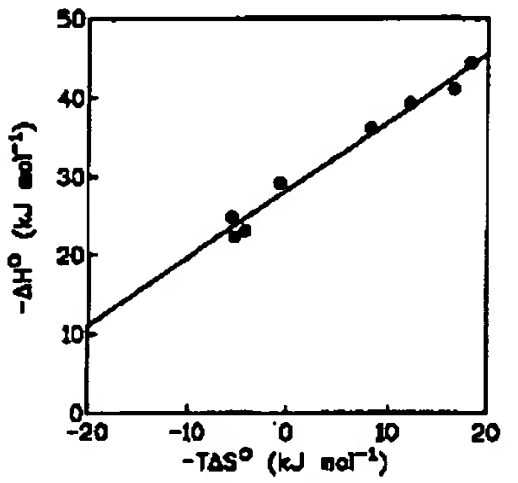

FIGURE 7: Enthalpy–entropy compensation plot for wild-type and mutant Se155-4 Fabs. The straight line was obtained by linear regression and has slope of 0.863 with an intercept of 28.3 kJ mol^{-1} ($r = 0.989$).

but possess many of the features of the periplasmic receptors, such as the aromatic residue stacking phenomenon and a reliance on hydrogen bonds. With respect to hydrogen-bond type, the carbohydrate recognition site of the Se155-4 antibody is somewhat unusual in that there is a lack of carboxylate and amide side-chain involvement in the hydrogen-bond network (Cygler et al., 1991). Instead, histidine side-chain, tryptophan side-chain, and backbone interactions dominate the hydrogen-bonding scheme. The stacking of aromatic side chains against the sugar ring is thought to discriminate against antigens carrying dideoxyhexoses other than abequose. Antigen mapping studies by functional group replacements (Bundle et al., unpublished results) have shown that the binding site fails to bind such antigens.

The His^{101H} mutagenesis results obtained for Se155-4 revealed that a number of interrelated factors are involved in the contribution of this residue to binding. The His^{101H}Glu and His^{101}Gln mutants displayed significantly higher enthalpy changes associated with trisaccharide binding. This is indicative of improved hydrogen-bond and/or van der Waals contacts. However, there was also a dramatic shift in the entropy term which more than offset the enthalpy gain. This result can be explained in different ways, but all point to the excellent balance between surface complementarity and hydrogen-bonding possibilities provided by the histidine side chain. The Glu and Gln substitutions may have resulted in the introduction of an additional hydrogen bond but the associated motional restrictions led to a net negative effect on affinity, because of a highly unfavorable entropy term. The formation of a bidentate hydrogen bond involving mannose and the Glu side chain is easily envisioned (Figure 6). Replacement of His^{101H} by dicarboxylic acids or the corresponding amides could potentially allow for simultaneous hydrogen bonding to both O-4 and O-6 of the mannose residue. Hydrogen bonding of this type has been observed in several carbohydrate–protein complexes and may require the participation of a bound water molecule acting as either a hydrogen-bond donor or acceptor (Vyas, 1991). Alternatively, the large negative entropy change could be the result of a loss of surface complementarity allowing one or more additional water molecules to be trapped in the complex. The thermodynamic behavior of His^{101H}Asn and His^{101H}Asp was similar to that of the wild type. The side chain of Asn can be superimposed on the imidazole ring of histidine so that the amido group occupies the same position as the π-N of the imidazole ring, whereas the equivalent amido group of Gln may be superimposed on the τ-N of the ring. These results offer evidence that the π-N of the histidine is the one that forms the hydrogen bond with O-4 mannose.

All of the His^{101H} mutants were characterized by an enthalpy–entropy compensation effect as shown by the linear relationship that exists for changes in the two terms for each mutant (Figure 7). Enthalpy–entropy compensation has previously been demonstrated in studies on the effects of the degree of ligand polymerization (Sigurskjold et al., 1991) and temperature (Sigurskjold & Bundle, 1992) on antigen binding by Se155-4. Strong enthalpy–entropy compensation has also been reported for three monoclonal anti-fluorescyl antibodies (Herron et al., 1986). Binding of the ligand by the wild type is predominantly enthalpy driven with some favorable assistance from entropy. This is somewhat atypical for sugar binding to proteins, where entropy is usually unfavorable. The source of the favorable entropy contribution is the efficient displacement of water molecules from the interacting surfaces of the protein binding site and the ligand. Changes in enthalpy and entropy always tend to compensate each other to some degree. For instance, if an enthalpic interaction is lost (e.g., a salt-bridge, a hydrogen bond, or a van der Waals interaction), an amount of entropy will be gained from this due to increased motional freedom and, conversely, increased motional restrictions will be introduced if a new binding interaction is formed. In aqueous solution, a substantial part of the enthalpy–entropy compensation comes from solvent displacement. When water molecules arrange themselves around the

surface of a solute (especially around hydrophobic surfaces), they form ordered structures with enthalpically stronger hydrogen bonds compensated by loss of entropy. When these molecules are stripped off upon binding, an amount of enthalpy is lost, compensated by an increase in entropy. If a group of analogous species interact by the same mechanism, then a linear relationship between enthalpy and entropy can be expected (Leffler & Grunwald, 1963). This linear relationship determines the extent of the compensation between ΔH° and $-T\Delta S^\circ$. The Fab mutants described here all lie on the same line of compensation with a slope of 0.86. A slope of less than 1 (complete compensation) means that the free energy correlates with entropy; i.e., the binding becomes stronger as $-T\Delta S^\circ$ becomes more negative. It follows from the van't Hoff relation, $\delta(\ln K)/\delta T = \Delta H^\circ/(RT^2)$, that when $\Delta H^\circ = 0$, the binding constant K is at its maximum. By extrapolation of the compensation plot, this occurs at $-T\Delta S^\circ = \Delta G^\circ = -32.8$ kJ mol^{-1}, which corresponds to $K = 5.0 \times 10^5$ M^{-1}. This K can be viewed as the maximum achievable for this particular ligand at 25 °C. It is seen that K for the wild type is reasonably close to this value but that it might be possible by further mutation to increase the affinity by a factor of 2. Interestingly, the highest K found in a study of the temperature dependence of ligand binding by Se155-4 was also 5.0×10^5 M^{-1}, occurring at 18 °C (Sigurskjold & Bundle, 1992).

An unusual number of the H3 residues of Se155-4 form backbone interactions with antigen. In the His^{101H}Gly mutant, the only H3 side-chain hydrogen bond to antigen was removed with surprisingly little effect on binding. A very favorable enthalpy term for this mutant suggested that a strong main-chain interaction had been introduced at position 101H. With this change, five of the nine H3 residues are glycine and four are contiguous in the sequence. This highly flexible structure should permit reorientation to allow a new interaction, and the unfavorable entropy term is consistent with this interpretation of the results. It is not possible, however, to exclude the explanation that the introduction of water-mediated hydrogen bonds accounts for the dramatically increased enthalpy contribution to binding. In either case, the data once again illustrate the enthalpy–entropy compensation effect (Figure 7) that may explain the difficulty in obtaining affinity increases in proteins already possessing good carbohydrate-binding properties (Vermersch et al., 1990, 1991). Gly^{102H} was found to be irreplaceable. Its backbone conformation is absolutely crucial because of the involvement of its NH in forming a hydrogen-bond network with the hydroxyl groups at *O*-2-abequose, *O*-2-galactose, and *O*-1-abequose. The frequent occurrence of Gly residues in CDR-H3s, as shown by reading frame preferences (Abergel & Claverie, 1991), is therefore not due entirely to their flexible nature but may reflect the roles of backbone H-bonding in antigen binding. Tyr^{103H}, a residue at the interface between the V_L and V_H domains, could be replaced only by alkyl/hydrophobic side chains, thus defining its role in the hydrophobic interaction between domains.

The CDR-H3 has a more complex origin than the other CDRs, deriving from the D-segment along with junctional and N-variability. It shows greater variability also as underlined by the Wu/Kabat plots of mouse H-chain variability (Wu & Kabat, 1970). These features point to this portion of the antibody combining site having greater importance in antigen recognition. The mutation data nevertheless show that binding activity is retained in a wide range of mutants with only one residue, Gly^{102H}, being irreplaceable. Thus, the natural process of somatic mutation in most cases would not result in loss of activity, and this robustness has obvious advantages in the efficiency of somatic mutations to produce affinity improvements.

The results presented here once again draw attention to the crucial role that framework residue Arg^{98H} (position 94H in the Kabat numbering system) can play in H3 conformation. Changes to this residue have altered the binding characteristics of anti-digoxin (Panka et al., 1988; Novotny et al., 1990) and anti-phosphorylcholine (Chien et al., 1989) antibodies. It is generally assumed that it exerts its structural role by formation of a salt-bridge with Asp^{106H} (position 101H in the Kabat numbering system). In support of this, Tempest et al. (1991) have observed that the grafting of a murine H3 from an antibody lacking arginine at this position was successful only if the arginine at this position in the human framework was substituted. It is clear that a positive charge at heavy-chain position 98 is an essential feature of Se155-4. The requirement for a negative charge at position 106H is less stringent, suggesting that the role of Arg^{98H} is not limited to the formation of the Arg^{98H}–Asp^{106H} salt-bridge. An understanding of how framework structure affects hypervariable loop conformation and of the atomic interactions between loop residues and bound antigen will form the basis of successful antibody engineering. For example, the humanizing of murine monoclonal antibodies by grafting murine CDRs on human frameworks will not work if loop conformation is distorted in the process; compatible frameworks must be identified or engineered (Foote & Winter, 1992).

The blocking of affinity increases by entropy effects and the influence of framework changes on antigen binding thermodynamics emphasize the limitations of predictive redesign of antibodies, even when three-dimensional details of antigen and antibody structure are known. The generation of random mutations, coupled with the emerging phage display technology that enables selection for rare mutants from huge libraries (Barbas et al., 1991; Marks et al., 1991; Narang et al., unpublished results), may be a preferred route for tailoring the binding properties of antibodies to meet different requirements.

ACKNOWLEDGMENT

We thank Dr. X. Ma for help with designing the mutagenesis strategy, Dr. Steve Evans for help with the stereo diagrams, and Mr. V. Tuli for technical assistance. NRCC no. 34296.

REFERENCES

Abergel, C., & Claverie, J.-M. (1991) *Eur. J. Immunol. 21*, 3021–3025.

Alt, F. W., & Baltimore, D. (1982) *Proc. Natl. Acad. Sci. U.S.A. 79*, 4118–4122.

Alzari, P. M., Lascombe, M.-B. & Poljak, R. J. (1988) *Annu. Rev. Immunol. 6*, 555–580.

Anand, N. N., Dubuc, G., Mandal, S., Phipps, J., Gidney, M. A. J., Sinnott, B., Young, N. M., MacKenzie, C. R., Bundle, D. R., & Narang, S. A. (1990) *Protein Eng. 3*, 541–546.

Anand, N. N., Dubuc, G., Phipps, J., MacKenzie, C. R., Sadowska, J., Young, N. M., Bundle, D. R., & Narang, S. A. (1991a) *Gene 100*, 39–44.

Anand, N. N., Mandal, S., MacKenzie, C. R., Sadowska, J., Sigurskjold, B., Young, N. M., Bundle, D. R., & Narang, S. A. (1991b) *J. Biol. Chem. 266*, 21874–21879.

Barbas, C. F., Kang, A. S., Lerner, R. A., & Benkovic, S. J. (1991) *Proc. Natl. Acad. Sci. U.S.A. 88*, 7978–7982.

Better, M., Chang, C. P., Robinson, R. R., & Horwitz, A. H. (1988) *Science 240*, 1041–1043.

Bundle, D. R., & Young, N. M. (1992) *Curr. Opin. Struct. Biol. 2*, 666–673.
Chien, N. C., Roberts, V. A., Giusti, A. M., Scharff, M. D., & Getzoff, E. D. (1989) *Proc. Natl. Acad. Sci. U.S.A. 86*, 5532–5536.
Chothia, C., & Leak, A. M. (1987) *J. Mol. Biol. 196*, 901–917.
Cygler, M., Rose, D. R., & Bundle, D. R. (1991) *Science 253*, 442–445.
Feizi, T. (1991) *Curr. Opin. Struct. Biol. 1*, 766–770.
Foote, J., & Winter, G. (1992) *J. Mol. Biol. 224*, 487–499.
Herron, J. N., Kranz, D. M., Jameson, D. M. & Voss, E. W. (1986) *Biochemistry 25*, 4602–4609.
Leffler, J. E., & Grunwald, E. (1963) *Rates and Equilibria of Organic Reactions*, Wiley, New York.
Marks, J. D., Hoogenboom, H. R., Bonnert, T. P., McCafferty, J., Griffiths, A. D., & Winter, G. (1991) *J. Mol. Biol. 222*, 581–597.
Mian, I. S., Bradwell, A. R., & Olson, A. J. (1991) *J. Mol. Biol. 217*, 133–151.
Narang, S. A., Yao, F. L., Michniewicz, J. J., Dubuc, G., Phippa, J., & Somorjai, R. L. (1987) *Protein Eng. 1*, 481–485.
Narang, S. A., Brummell, D. A., Sharma, V., Dubuc, G., MacKenzie, C. R., Michniewicz, J., Sadowska, J., Anand, N., Young, N. M., & Bundle, D. R. (1991) *Nucleic Acids Res. Symp. Ser. 24*, 173–179.
Novotny, J., Bruccoleri, R. E., & Haber, E. (1990) *Proteins: Struct., Funct. Genet. 7*, 93–98.
Panka, D. J., Mudgett-Hunter, M., Parks, D. R., Peterson, L. L., Herzenberg, L. A., Haber, E., & Marjolies, M. N. (1988) *Proc. Natl. Acad. Sci. U.S.A. 85*, 3080–3084.
Quiocho, F. A. (1991) *Curr. Opin. Struct. Biol. 1*, 922–933.
Sambrook, J., Fritsch, E. F., & Maniatis, T. (1989) *Molecular Cloning: A Laboratory Manual*, 2nd ed., Cold Spring Harbor Laboratory, Cold Spring Harbor, NY.
Sigurskjold, B. W., & Bundle, D. R. (1992) *J. Biol. Chem. 267*, 8371–8376.
Sigurskjold, B. W., Altman, E., & Bundle, D. R. (1991) *Eur. J. Biochem. 197*, 239–246.
Skerra, A., & Plückthun, A. (1988) *Science 240*, 1038–1040.
Spurlino, J. C., Lu, G.-Y., & Quiocho, F. A. (1991) *J. Biol. Chem. 266*, 5202–5219.
Svenson, S. B., & Lindberg, A. A. (1978) *J. Immunol. 120*, 1750–1758.
Takeo, K., & Kabat, E. A. (1978) *J. Immunol. 121*, 2305–2310.
Takeo, K., & Nakamura, S. (1972) *Arch. Biochem. Biophys. 153*, 1–7.
Tempest, P. R., Bremner, P., Lambert, M., Taylor, G., Furze, J. M., Carr, F. J., & Harris, W. J. (1991) *Bio/Technology 9*, 266–271.
Vermersch, P. S., Tesmer, J. J. G., Lemon, D. D., & Quiocho, F. A. (1990) *J. Biol. Chem. 265*, 16592–16603.
Vermersch, P. S., Lemon, D. D., Tesmer, J. J. G., & Quiocho, F. A. (1991) *Biochemistry 30*, 861–866.
Vyas, N. K. (1991) *Curr. Opin. Struct. Biol. 1*, 732–740.
Vyas, N. K., Vyas, M. N., & Quiocho, F. A. (1991) *J. Biol. Chem. 266*, 5226–5237.
Wiseman, T., Williston, S., Brandts, J. F., & Lin, L.-N. (1989) *Anal. Biochem. 17*, 131–137.
Wu, T. T., & Kabat, E. A. (1970) *J. Exp. Med. 132*, 211–250.

Protein Engineering vol.12 no.10 pp.879–884, 1999

Tryptophan H33 plays an important role in pyrimidine (6–4) pyrimidone photoproduct binding by a high-affinity antibody

Hiroyuki Kobayashi, Jiro Kato, Hiroshi Morioka, Jon D.Stewart[1] and Eiko Ohtsuka[2]

Graduate School of Pharmaceutical Sciences, Hokkaido University, Kita-ku, Sapporo 060-0812, Japan and [1]Department of Chemistry, University of Florida, Gainesville, FL 32611, USA

[2]To whom correspondence should be addressed; email: ohtsuka@pharm.hokudai.ac.jp

The importance of Trp H33 in antibody recognition of DNA containing a central pyrimidine (6–4) pyrimidone photoproduct was investigated. This residue was replaced by Tyr, Phe and Ala and the binding abilities of these mutants were determined by surface plasmon resonance and fluorescence spectroscopy. Conservative substitution of Trp H33 by Tyr or Phe resulted in moderate losses of binding affinity; however, replacement by Ala had a significantly larger impact. The fluorescence properties of DNA containing a (6–4) photoproduct were strongly affected by the identity of the H33 residue. DNA binding by both the wild-type and the W-H33-Y mutant was accompanied by a small degree of fluorescence quenching; by contrast, binding by the W-H33-F and W-H33-A mutants produced large fluorescence increases. Taken together, these variations in binding and fluorescence properties with the identity of the H33 residue are consistent with a role in photoproduct recognition by Trp H33 in the high-affinity antibody 64M5.

Keywords: antibodies/fluorescence/mutagenesis/pyrimidine (6–4) pyrimidone photoproduct/surface plasmon resonance

Introduction

Pyrimidine (6–4) pyrimidone dimers are major products of DNA photodamage that have been associated with mutation and cell death in the absence of repair (Friedberg *et al.*, 1995; Sancar, 1996; Wood, 1996). *In vivo*, (6–4) photoproducts are detected and corrected efficiently by enzymes of the excision repair pathway (Jones and Wood, 1993). Because they have very high binding affinities and specificities that can be programmed by proper choice of the immunogen, monoclonal antibodies have also been explored as a means to detect and quantitate these photolesions (Roza *et al.*, 1988; Mizuno *et al.*, 1991; Mori *et al.*, 1991; Matsunaga *et al.*, 1993). While the three-dimensional structures of antibodies and repair proteins are undoubtedly quite different, it is possible that both utilize similar features to distinguish photodamage lesions in the presence of a vast excess of normal B-helical DNA. We have therefore studied a series of murine monoclonal antibodies raised against UV-irradiated calf thymus DNA (Mori *et al.*, 1991). Four of these antibodies were specific for DNA containing pyrimidine (6–4) pyrimidone photoproducts in both single- and double-stranded DNA. The variable region genes for these four anti-(6–4) photoproduct antibodies have been cloned and sequenced (Morioka *et al.*, 1998). Three of the four sequences (antibodies 64M2, 64M3 and 64M5) are highly related to one another; however, the 64M5 antibody binds antigen at least an order of magnitude more tightly than the 64M2 and 64M3 antibodies (Mori *et al.*, 1991).

A variety of techniques have been used to examine the details of protein–DNA interactions in the series of anti-(6–4) photoproduct antibodies. Computer modeling predicted that the Fv structures of antibodies 64M2, 64M3 and 64M5 would be highly similar and that interactions with the (6–4) photoproduct itself would involve mainly non-charged interactions since the center of the combining site was predicted to possess few ionizable amino acid side chains (Morioka *et al.*, 1998). On the other hand, it was observed experimentally that the affinity of the 64M5 antibody for oligonucleotides containing a central (6–4) photoproduct increased with increasing lengths up to a hexanucleotide (Kobayashi *et al.*, 1998a). This suggests that electrostatic contacts might be formed between antibody side chains and phosphate groups on flanking regions of the oligonucleotides and these have been detected experimentally by ^{31}P NMR (Torizawa *et al.*, 1998). A strongly cationic patch was observed on the 64M5 VH surface approximately 20 Å from the center of the combining site. Single and multiple alanine replacements for the four lysine residues making up this cationic patch were created and the properties of these mutants suggested that the region functioned in the wild-type protein as an 'electrostatic steering' element during the association phase of DNA binding, although these amino acid side chains apparently did not interact directly with the antigen after binding had occurred (Kobayashi *et al.*, 1998b). Mutagenesis studies of CDR loop amino acids that differed between the 64M5 and 64M2 antibodies suggested that these proteins undergo conformational changes upon antigen binding and that the greater propensity to undergo these conformational changes is the major reason for the higher affinity of the 64M5 antibody (Kobayashi *et al.*, 1999). The X-ray crystal structures of the free 64M5 Fab fragment and the 64M2 Fab fragment complexed with a d(TT) (6–4) photoproduct dimer have been solved recently (Yokoyama,H., Mizutami,R., Satow,Y., Komatsu,Y., Ohtsuka,E. and Nikaido,O., manuscript in preparation). These experimental structures were very similar to those predicted by computer modeling and comparison of the bound and free states showed the conformational changes expected from earlier studies. The apparent stacking interaction between the Trp H33 side chain and the 3′ pyrimidone nucleotide was a particularly striking feature of the 64M2 complex structure (Figure 1). This Trp residue, located in VH CDR1, is conserved in the 64M2, 64M3 and 64M5 antibodies and also in a number of other murine anti-DNA antibodies of the γ2a and γ2b subclasses (Kabat *et al.*, 1992).

Stacking interactions between indole rings and nucleoside bases have been implicated in a variety of protein–DNA interactions. NMR studies have demonstrated such interactions with undamaged DNA in both model peptides (Sartorius and Schneider, 1995) and the HIV capsid protein (Morellet *et al.*,

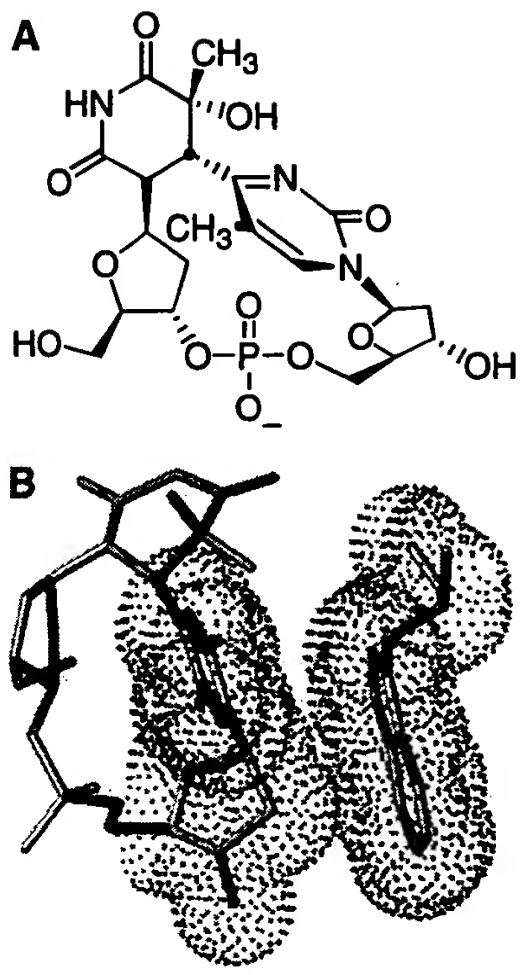

Fig. 1. Pyrimidine (6–4) pyrimidone photoproduct and its interaction with the 64M2 antibody. (**A**) Structure of the d(TT) (6–4) photoproduct. (**B**) Contact between the 64M2 Trp H33 side chain and the 3′ pyrimidone of the bound (6–4) photodimer. These coordinates were taken from the X-ray structure of this complex, which was prepared by co-crystallization with the photodimer shown in (A). Heavy atoms of both the protein and DNA are shown as heavy gray lines and the van der Waals surface of both Trp H33 and the pyrimidone portion of the photoproduct are indicated by black dots.

1998). These interactions have also been observed in damaged DNA recognition. Pi-stacking interactions between indole and methylated adenine derivatives have been investigated by small-molecule X-ray crystallography (Ishida *et al.*, 1983; Yamagata *et al.*, 1994) as models for the repair enzyme 3-methyladenine DNA glycosylase, whose crystal structure in a complex with DNA has been recently determined (Lau *et al.*, 1998). A π-stacking role for a tryptophan side chain has also been proposed for *Escherichia coli* exonuclease III (AP endonuclease VI) (Shida *et al.*, 1996).

In this paper, we examine the role of Trp H33 in photoproduct binding by the 64M5 scFv. Mutants were constructed in which this residue was substituted with phenylalanine, tyrosine or alanine. While the W-H33-F and W-H33-Y mutants retained a large fraction of the wild-type binding affinity for DNA's containing a (6–4) photoproduct, the W-H33-A substitution dramatically diminished antigen binding. Pyrimidine (6–4) pyrimidone photoproducts are fluorescent, and this property was exploited to probe the local environment of the bound antigen in the wild-type and the mutant scFvs. Taken together, our results indicate that Trp H33 plays a key role in DNA photoproduct binding by the 64M5 antibody, most likely by π-stacking interactions.

Materials and methods

General

Restriction and DNA modifying enzymes were purchased from Takara Shuzo, New England Biolabs, Bethesda Research Labs, Stratagene, Toyobo or Boehringer Mannheim. Reagents were obtained from Wako Pure Chemical Industries, Nacalai Tesque or Sigma Chemical and were used as received. DNA phosphoramidite reagents were obtained from Perkin Elmer Applied Biosystems. Routine cloning was performed according to Sambrook *et al.* (1989).

Preparation of oligonucleotides

Solid-phase oligonucleotide synthesis was carried out on an Applied Biosystems Model 394 DNA/RNA synthesizer using standard β-cyanoethyl chemistry according to the manufacturer's protocol. Oligonucleotides were purified for surface plasmon resonance measurements by reversed-phase HPLC (μBondapak C18, Waters). Those used for molecular biology techniques were purified by denaturing polyacrylamide gels. 3′-Biotinylated oligonucleotides containing a (6–4) photoproduct (T[6–4]T and CAAT[6–4]TAAG) were prepared as described previously (Kobayashi *et al.*, 1998a).

Production and isolation of mutant 64M5 scFv's

Trp H33 was replaced by alanine, phenylalanine and tyrosine using PCR methods (Higuchi, 1989) and detailed procedures have been described previously (Kobayashi *et al.*, 1999). All mutant DNA sequences were confirmed by automated DNA sequencing (Applied Biosystems Model 373A). Once constructed, each mutant scFv gene was introduced into an expression plasmid in which the scFv was fused to a hexahistidine tag (Kobayashi *et al.*, 1999).

All of the scFv's accumulated in *Escherichia coli* cells in the form of inclusion bodies according to SDS–PAGE and western blotting. Active proteins were obtained by solubilizing the inclusion bodies in 6 M guanidinium hydrochloride followed by an on-column refolding and purification procedure (Kobayashi *et al.*, 1999). The scFv's were further purified by gel filtration using a Superose 12 HR 10/30 column equilibrated with HBS (10 mM HEPES, pH 7.4, 150 mM NaCl, 3.4 mM EDTA, 0.005% Tween-20) using a SMART-system (Pharmacia Biotech).

Surface plasmon resonance determination of (6–4) photoproduct binding by scFv's

Binding of scFv's to oligonucleotides containing a (6–4) photoproduct was measured by surface plasmon resonance (SPR) measurements using a BIAcore instrument as described previously (Kobayashi *et al.*, 1999). The minimal amount of DNA was immobilized on the sensor chip in order to avoid mass transport limitations. Injections of biotinylated oligonucleotides (0.01 pmol/μl in HBS) were repeated until the SPR signal was increased by 10–30 resonance units (RU) above the original baseline. Purified scFv's were diluted in HBS buffer, then they were injected over the immobilized oligonucleotides at a flow rate of 100 μl/min over a concentration range from 10 to 200 nM. Sensorgrams were recorded and normalized to a base line of 0 RU. Equivalent volumes of diluted antibodies were also injected over a non-oligonucleotide surface to serve as blank sensorgrams to allow subtraction of the bulk refractive index background. The association was monitored by measuring the rate of binding to antigen at different protein concentrations. The dissociation of these antibodies from the antigen surface was monitored after the end of the association phase. The remaining bound antibodies were removed completely by injecting 50–100 μl 100 mM HCl. Kinetic rate constants were calculated using BIAevaluation 2.1 software (Biacore) using a single-site binding model (A + B = AB). The ratio of the

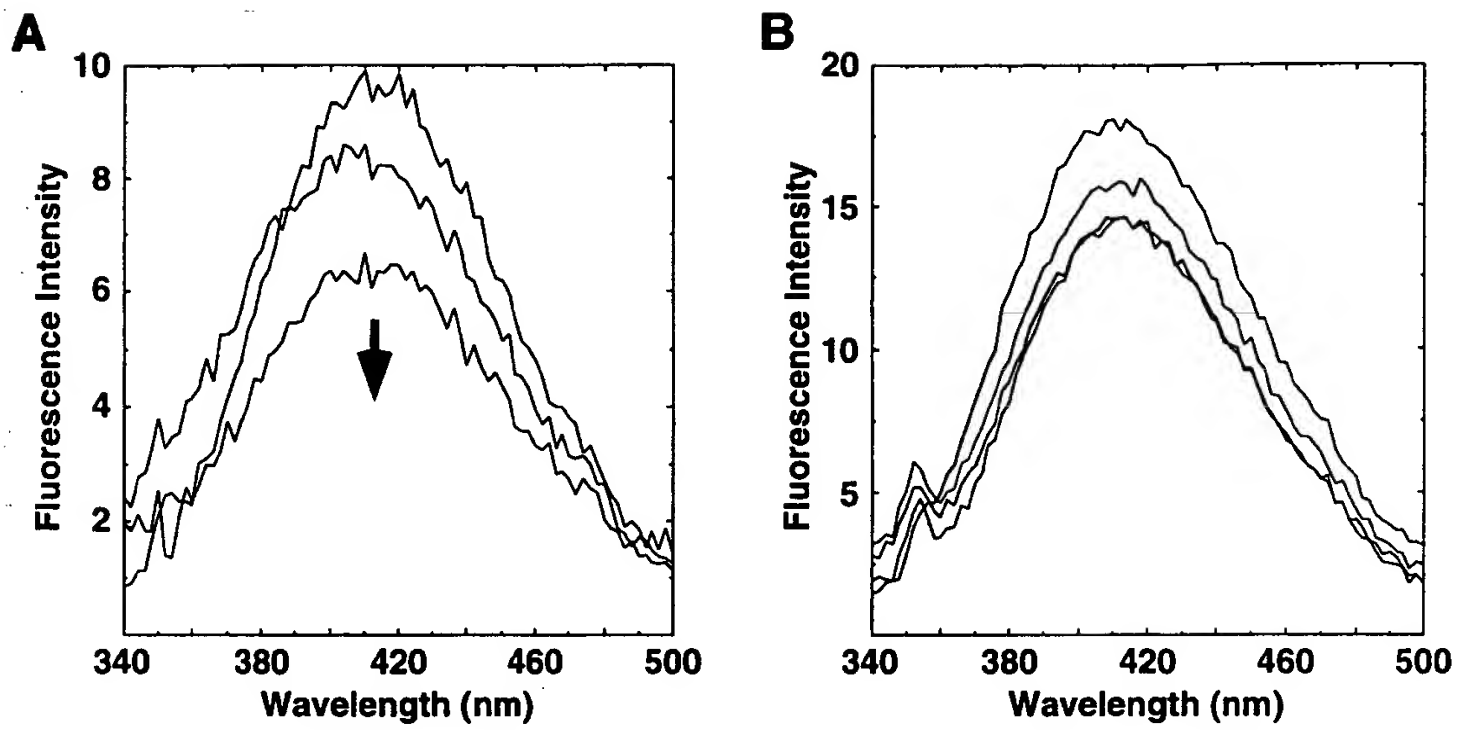

Fig. 2. Fluorescence emission spectra of the (6–4) photoproduct with excitation at 313 nm in the presence of wild-type 64M5 scFv. (**A**) Emission spectrum of 200 pmol [5′-d(CAAT(6–4)TAAG)-3′] in the presence of 0, 100 and 200 pmol wild-type 64M5 scFv. (**B**) Emission spectrum of 50 pmol [5′-d(T(6–4)T)-3′] in the presence of 0, 25, 50 and 100 pmol wild-type 64M5 scFv. No clear trend in intensity changes as a function of added scFv was observed in this case.

Table I. Kinetic constants for the binding of scFv's to oligonucleotides containing a (6–4) photoproduct

scFv	d2-mer-(6–4)[a]			d8-mer-(6–4)[b]		
	k_{ass} ($M^{-1}s^{-1}$)	k_{diss} (s^{-1})	k_{diss}/k_{ass} (M)	k_{ass} ($M^{-1}s^{-1}$)	k_{diss} (s^{-1})	k_{diss}/k_{ass} (M)
Wild type[c]	$(9.5\pm0.7)\times10^{5}$	$(1.5\pm0.2)\times10^{-3}$	$1.6\pm0.2)\times10^{-9}$	$(1.1\pm0.1)\times10^{6}$	$(1.1\pm0.2)\times10^{-4}$	$(1.0\pm0.1)\times10^{-10}$
W-H33-Y	$(9.0\pm0.1)\times10^{4}$	$(4.4\pm0.4)\times10^{-3}$	$(4.9\pm0.4)\times10^{-8}$	$(4.8\pm0.3)\times10^{5}$	$(2.1\pm0.1)\times10^{-4}$	$(4.4\pm0.3)\times10^{-10}$
W-H33-F	$(1.9\pm0.3)\times10^{4}$	$(8.4\pm0.3)\times10^{-3}$	$(4.4\pm0.7)\times10^{-7}$	$(4.5\pm0.1)\times10^{5}$	$(2.1\pm0.1)\times10^{-4}$	$(4.7\pm0.2)\times10^{-10}$
W-H33-A	ND	ND	–	$(1.3\pm0.6)\times10^{5}$	$(1.0\pm0.1)\times10^{-2}$	$(8.0\pm4.0)\times10^{-8}$

[a]d(T<6–4>T).
[b]d(CAAT<6–4>TAAG).
[c]Kobayashi *et al.* (1999).
ND, No binding detected under standard conditions.

rate constants allowed the apparent equilibrium constant to be calculated, $K_{D,app} = k_{diss}/k_{ass}$.

Fluorescence measurements of (6–4) photoproduct with scFv's

Steady-state fluorescence excitation and emission spectra of (6–4) photoproduct with scFv's were measured on a Model FP-777 spectrofluorometer (Japan Spectroscopic Co, Ltd) using a 6 mm square cuvette and a sample volume of 200 μl. The emission spectra were recorded over the wavelength range from 250 to 500 nm with an excitation wavelength of 313 nm. The spectral bandpass was 5 nm for all emission spectra. After obtaining the emission scan for the photoproduct-containing oligonucleotides alone in a HBS buffer, scFv proteins were added at the indicated concentrations and allowed to equilibrate for 30 min at 25°C prior to spectral measurements.

Results

A tryptophan at position H33 is present in all three closely-related anti-(6–4) photoproduct antibodies (64M2, 64M3 and 64M5). Moreover, the three-dimensional structures of the 64M2 and 64M5 Fab fragments determined by X-ray crystallography are highly similar (Yokoyama,H., Mizutami,R., Satow,Y., Komatsu,Y., Ohtsuka,E. and Nikaido,O., manuscript in preparation). We therefore chose to investigate the role of Trp H33 in the context of the 64M5 scFv since this antibody has the highest affinity for photoproduct-containing oligonucleotides (Mori *et al.*, 1991) and because of our previous experience in site-directed mutagenesis studies of the 64M5 scFv (Kobayashi *et al.*, 1998b, 1999). We expect the role of Trp H33 to be identical in antigen binding by the 64M2, 64M3 and 64M5 antibodies. All scFv's used in this study had the VL–linker–VH–His_6 structure that better reproduces the binding properties of the native 64M5 monoclonal antibody and the proteolytically-prepared Fab fragment (Kobayashi *et al.*, 1999).

We replaced Trp H33 by Ala, Phe and Tyr using standard site-directed mutagenesis techniques (Higuchi, 1989) and expressed the scFv proteins along with C-terminal hexahistidine tags in *E.coli* as inclusion bodies. The pure scFv proteins were prepared by solubilizing the inclusion bodies with denaturant, capturing the unfolded proteins on metal affinity columns, then re-folding the scFv proteins while still attached to the solid support (Kobayashi *et al.*, 1999). After elution from the metal affinity column, the scFv's were further purified by gel filtration chromatography. The final chromatography step also indicated that the wild-type and all three mutant scFv's were predominantly monomeric under the experimental conditions.

The rate constants for photoproduct binding by the scFv's were determined by surface plasmon resonance and the data are summarized in Table I. Two DNA's were used: the (6–4) photodimer and an octanucleotide that contained a central

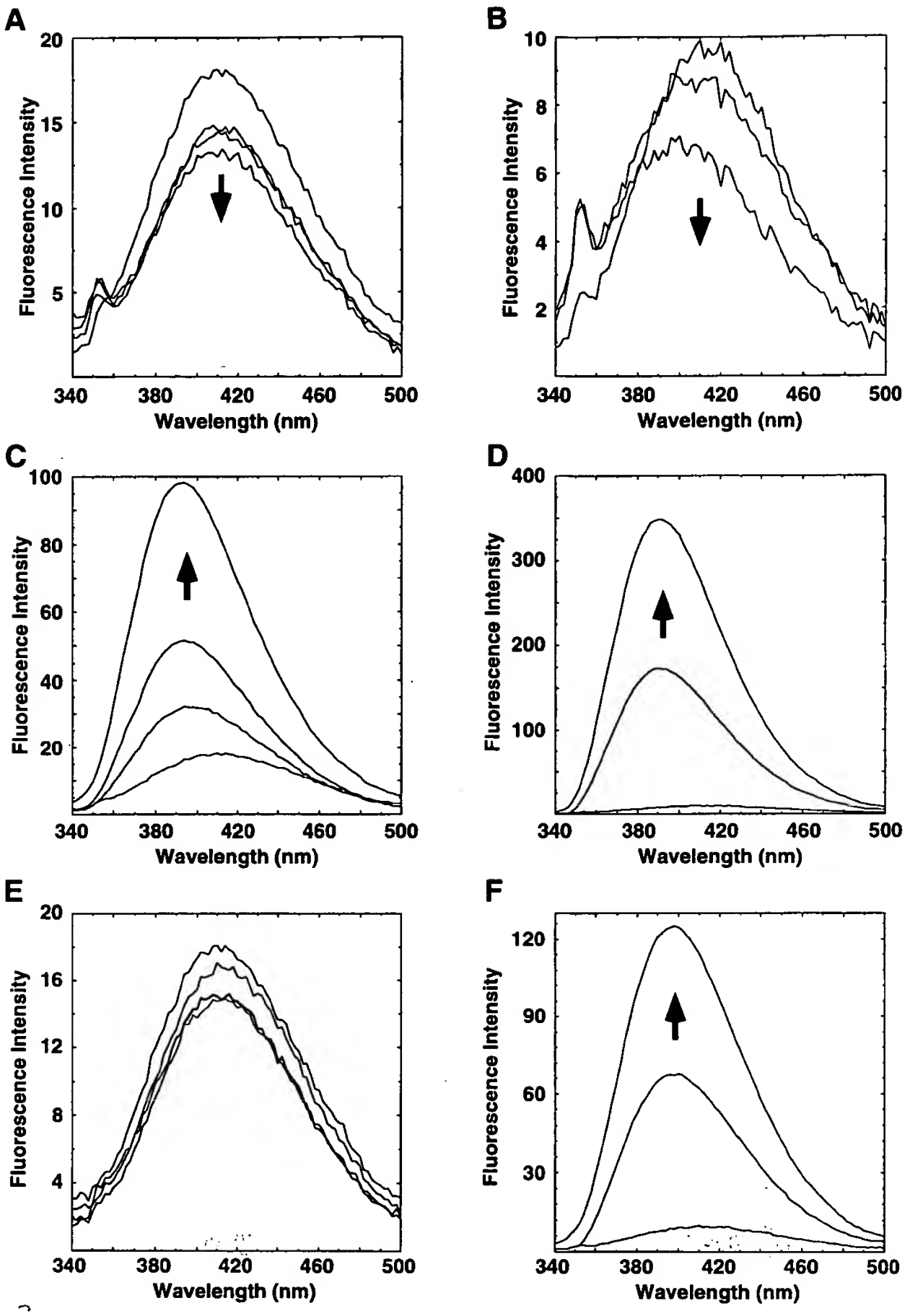

Fig. 3. Fluorescence emission spectra of the (6–4) photoproduct with excitation at 313 nm in the presence of mutant 64M5 scFv's. When observable, trends in intensity changes as a function of added scFv are indicated by arrows. (**A**) Emission spectrum of 50 pmol [5′-d(T(6–4)T)-3′] in the presence of 0, 25, 50 and 100 pmol W-H33-Y 64M5 scFv. (**B**) Emission spectrum of 200 pmol [5′-d(CAAT(6–4)TAAG)-3′] in the presence of 0, 100 and 200 pmol W-H33-Y 64M5 scFv. (**C**) Emission spectrum of 50 pmol [5′-d(T(6–4)T)-3′] in the presence of 0, 25, 50 and 100 pmol W-H33-F 64M5 scFv. (**D**) Emission spectrum of 200 pmol [5′-d(CAAT(6–4)TAAG)-3′] in the presence of 0, 100 and 200 pmol W-H33-F 64M5 scFv. (**E**) Emission spectrum of 50 pmol [5′-d(T(6–4)T)-3′] in the presence of 0, 25, 50 and 100 pmol W-H33-A 64M5 scFv. (**F**) Emission spectrum of 200 pmol [5′-d(CAAT(6–4)TAAG)-3′] in the presence of 0, 100 and 200 pmol W-H33-A 64M5 scFv.

(6–4) photoproduct. The former was designed to probe interactions with the photoproduct itself while the latter would also allow contributions to binding energy by contacts with flanking nucleotides. The W-H33-A mutant was unable to bind the dimer at detectable levels under our experimental conditions, although binding to the octamer was measurable.

The (6–4) photoproduct fluoresces with an emission maximum near 405 nm when excited at 313 nm (Hauswirth and Wang, 1977; Franklin *et al.*, 1982). Because the fluorescence properties depend on the relative torsional angle between the 5′-pyrimidine and the 3′-pyrimidone ring of the photoproduct, we exploited this technique to characterize DNA binding by the 64M5 scFv mutants. Figure 2 shows the emission spectra of the (6–4) photoproduct dimer and octamer used previously to characterize the scFv's by surface plasmon resonance. Stepwise addition of the wild-type 64M5 scFv caused a small

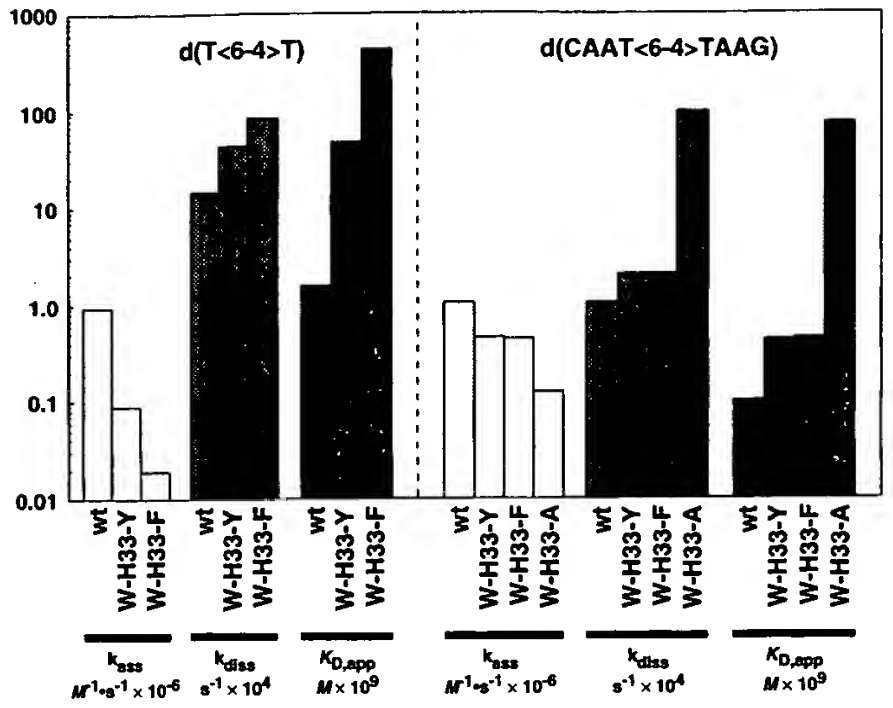

Fig. 4. Graphical representation of rate constants for photoproduct binding as determined by surface plasmon resonance.

progressive decrease in fluorescence intensity in the case of the octamer; however, only very slight changes were observed in the case of the dimer and no trend was apparent. In the case of the octamer, infinitely tight binding would be expected under the experimental conditions and the extent of fluorescence quenching as a function of added scFv was consistent with this expectation. Repeating this experiment with the W-H33-Y mutant gave similar results (Figure 3A and B). In the case of the octamer, infinitely tight binding was expected on the basis of the $K_{D,app}$ value determined by surface plasmon resonance and the data fit this expectation. In the case of the photoproduct dimer, both the DNA and the scFv concentrations were within an order of magnitude of the $K_{D,app}$ value. These data could be well described by a quadratic binding equation that incorporated the $K_{D,app}$ value determined by surface plasmon resonance (data not shown), demonstrating that both methods for detecting scFv–DNA interactions yielded consistent results and that the observed fluorescence changes are unlikely to be experimental artifacts.

When photodimer fluorescence spectra were determined in the presence of increasing concentrations of the W-H33-F mutant, large increases in fluorescence intensities were observed along with a pronounced blue shift (Figure 3C and D). Similar behavior was observed for the W-H33-A mutant (Figure 3F). These data were also consistent with quadratic binding equations incorporating $K_{D,app}$ values determined by surface plasmon resonance. Only small fluorescence changes were detected when the W-H33-A mutant was added to the (6–4) photodimer (Figure 3E), consistent with our inability to detect this interaction by surface plasmon resonance.

Discussion

While Trp commonly occurs at position H33 in anti-DNA antibodies, and it is conserved among all three closely-related anti-(6–4) photoproduct antibodies, a variety of other residues are also found in the Kabat database at this location including Ala, Phe and Tyr (Kabat *et al.*, 1992). All three H33 mutants retained the ability to bind (6–4) photoproduct-containing DNA, suggesting that the mutations did not drastically alter the native three-dimensional structure. The rate constants for (6–4) photoproduct binding by the wild-type and mutant scFv's are shown graphically in Figure 4. As would be expected for a residue that interacts strongly with the photoproduct itself, mutations of Trp H33 had the greatest impact on binding of the photodimer. The flanking nucleotides present in the octamer provide additional contacts independent of Trp H33 (Morioka *et al.*, 1998), and this reduces the impacts of all but the Ala mutation. The latter may be a special case, however, since the dramatic reduction in side chain volume may also affect the positioning of other nearby residues.

The energetic impact of removing Trp H33 on DNA binding is consistent with its proposed role in stacking with the photoproduct 3′-pyrimidone base and with the results of site-directed mutagenesis studies of Trp–DNA interactions in other proteins. For example, Voss and co-workers analyzed the consequences of mutating Trp H100A in anti-single-stranded DNA autoantibody BV04-01, whose side-chain had been shown by X-ray crystallography to stack against the central thymine base of bound d(T_3) (Rumbley *et al.*, 1993). The role and positioning of this residue is thus analogous to that of Trp H33 in our photoproduct antibodies. Substitution of Trp H100A in BV04-01 by Tyr or Phe led to decreases in K_D values of 22- and 44-fold, respectively (Rumbley *et al.*, 1993). The corresponding alterations in $K_{D,app}$ values for mutation of Trp H33 to Tyr and Phe in 64M5 are 31- and 280-fold, respectively. In the case of DNA repair protein *E.coli* photolyase, a tryptophan side chain (Trp 277) is positioned within the substrate binding pocket (Park *et al.*, 1995). While mutation of this residue to Phe or His had little effect on substrate binding, replacement by His or Arg diminished the affinity of the protein by 1000-fold (Li and Sancar, 1990).

The alterations in (6–4) photoproduct fluorescence properties with changes in the H33 residue are also consistent with a π-stacking interaction involving Trp H33. Each mutation was introduced into the X-ray crystal structure of the 64M5 scFv using computer modeling. Interestingly, the aromatic rings of both Tyr and Phe were predicted to overlap with the 3′-pyrimidone base more extensively than the indole side chain of Trp H33. While it is not possible to quantitatively interpret the fluorescence changes caused by the 64M5 scFv, we note that the decrease in (6–4) photoproduct fluorescence intensity caused by the wild type 64M5 scFv was identical to that observed for the proteolytically-prepared 64M5 Fab (data not shown), suggesting that this quenching is an intrinsic part of the binding interaction rather than an artifact of the scFv. However, we cannot determine whether these changes in fluorescence properties are due to changes in the relative angle between the pyrimidine and pyrimidone π-systems upon binding, resonance energy transfer to nearby π-systems or some other mechanism. It is clear that replacing Trp H33 with Phe or Ala alters the local environment of the (6–4) photodimer since binding is accompanied by large fluorescence increases that are not seen with the wild-type scFv.

In summary, the results of the present study argue that Trp H33 plays a key role in (6–4) photoproduct binding by the high-affinity 64M5 antibody. Whether enzymes that recognize and repair these photolesions will also utilize a similar interaction with the 3′-pyrimidone base remains to be determined.

Acknowledgements

We thank Dr Yoshinori Satow (University of Tokyo) for permission to use the coordinates of the crystal structures cited in this work and Drs Yasuo Komatsu (Hokkaido University), Koichi Kato (University of Tokyo) and Ichio Shimada (University of Tokyo) for valuable discussions. This work was

supported by Grants-in-Aid by the Monbusho International Scientific Research Program and by Specially Promoted Research funding from the Ministry of Education, Science, Culture and Sports of Japan.

References

Franklin,W.A., Lo,K.M. and Haseltine,W.A. (1982) *J. Biol. Chem.*, **257**, 13535–13543.

Friedberg,E.C., Walker,G.C. and Siede,W. (1995) In *DNA Repair and Mutagenesis*. ASM Press, Washington, DC.

Hauswirth,W., and Wang,S.Y. (1977) *Photochem. Photobiol.*, **25**, 161–166.

Higuchi,R. (1989) In Erlich,H.A. (ed.), *PCR Technology*. Stockton Press, New York, pp. 61–70.

Ishida,T., Shibata,M., Fujii,K. and Inoue,M. (1983) *Biochemistry*, **22**, 3571–3581.

Jones,C.J. and Wood,R.D. (1993) *Biochemistry*, **32**, 12096–12104.

Kabat,E.A., Wu,T.T., Perry,H.M., Gottesman,K.S. and Foeller,C. (1992) *Sequences of Proteins of Immunological Interest*, Release 5.0. National Institutes of Health, Bethesda, MD. The most up-to-date release can be found at http://www.immuno.bme.nwu.edu

Kobayashi,H., Morioka,H., Torizawa,T., Kato,K., Shimada,I., Nikaido,O. and Ohtsuka,E. (1998a) *J. Biochem.*, **123**, 182–188.

Kobayashi,H., Morioka,H., Nikaido,O., Stewart,J.D. and Ohtsuka,E. (1998b) *Protein Engng*, **11**, 1089–1092.

Kobayashi,H., Morioka,H., Tobisawa,K., Torizawa,T., Kato,K., Shimada,I., Nikaido,O., Stewart,J.D. and Ohtsuka,E. (1999) *Biochemistry*, **38**, 532–539.

Lau,A.Y., Scharer,O.D., Samson,L., Verdine,G.L. and Ellenberger,E. (1998) *Cell*, **95**, 249–258.

Li,Y.F. and Sancar,A. (1990) *Biochemistry*, **29**, 5698–5706.

Matsunaga,T., Hatakeyama,Y., Ohta,M., Mori,T. and Nikaido,O. (1993) *Photochem. Photobiol.*, **57**, 934–940.

Mizuno,T., Matsunaga,T., Ihara,M. and Nikaido,O. (1991) *Mutat. Res.*, **254**, 175–184.

Morellet,N., Demene,H., Teilleux,V., Huynh-Dinh,T., de Rocquigny,H., Fournie-Zaluski,M.C. and Roques,B.P. (1998) *J. Mol. Biol.*, **283**, 419–434.

Mori,T., Nakane,M., Hattori,T., Matsunaga,M., Ihara,M. and Nikaido,O. (1991) *Photochem. Photobiol.*, **54**, 225–232.

Morioka,H., Miura,H., Kobayashi,H., Koizumi,T., Fujii,K., Asano,K., Matsunaga,T., Nikaido,O., Stewart,J.D. and Ohtsuka,E. (1998) *Biochim. Biophys. Acta*, **1385**, 17–32.

Park,H.-W., Kim,S.-T., Sancar,A. and Deisenhofer,J. (1995) *Science*, **268**, 1866–1872.

Roza,L., Van der Wulp,K.J.M., Macfarlane,S.J., Lohman,P.H.M. and Baan,R.A. (1988) *Photochem. Photobiol.*, **48**, 627–633.

Rumbley,C.A., Denzin,L.K., Yanta,L., Tetin,S.Y. and Voss,E.W.,Jr (1993) *J. Biol. Chem.*, **268**, 13667–13674.

Sambrook,J., Fritsch,E.F. and Maniatis,T. (1989) *Molecular Cloning: A Laboratory Manual*, 2nd Edn. Cold Spring Harbor Laboratory Press, Cold Spring Harbor.

Sancar,A. (1996) *Annu. Rev. Biochem.*, **65**, 43–81.

Sartorius,J. and Schneider,H.J. (1995) *FEBS Lett.*, **374**, 387–392.

Shida,T., Noda,M. and Sekiguchi,J. (1996) *Nucleic Acids Res.*, **24**, 4572–4576.

Torizawa,T., Kato,K., Kimura,Y., Asada,T., Kobayashi,H., Komatsu,Y., Morioka,H., Nikaido,O., Ohtsuka,E. and Shimada,I. (1998) *FEBS Lett.*, **429**, 157–161.

Wood,R.D. (1996) *Annu. Rev. Biochem.*, **65**, 135–167.

Yamagata,Y., Kato,M. and Fujii,S. (1994) *Chem. Pharm. Bull.*, **42**, 2385–2387.

Received February 26, 1999; revised May 24, 1999; accepted June 21, 1999

Proc. Natl. Acad. Sci. USA
Vol. 94, pp. 412–417, January 1997
Biochemistry

In vitro scanning saturation mutagenesis of an antibody binding pocket

ELIZABETH A. BURKS*, GANG CHEN*, GEORGE GEORGIOU†‡, AND BRENT L. IVERSON*†

*Department of Chemistry and Biochemistry, †Molecular Biology Program, and ‡Department of Chemical Engineering, University of Texas, Austin, TX 78712

Communicated by Allen J. Bard, University of Texas, Austin, TX, November 12, 1996 (received for review September 10, 1996)

ABSTRACT **We have combined PCR mutagenesis with *in vitro* transcription/translation and ELISA for the rapid generation and characterization of antibody mutants. The PCR products are used directly as the template for the *in vitro* transcription/translation reactions and because no cloning steps are required, the *in vitro* saturation mutagenesis of one residue can be completed in duplicate within a week by a single investigator. *In vitro* scanning saturation mutagenesis was used to analyze the role and plasticity of six key contact residues (H:Tyr-33, H:Asn-35, H:Tyr-50, H:Trp-100, L:Val-94, and L:Pro-96) in the binding pocket of a single chain Fv antibody derived from the 26–10 monoclonal antibody. A total of 114 mutant antibodies were produced; all 19 substitutions at each of the 6 chosen positions. The mutants were analyzed for binding to digoxin, digitoxin, digoxigenin, and ouabain resulting in the generation of a comprehensive data base of 456 relative affinity values. Excellent agreement between the relative affinity values obtained with *in vitro* synthesized mutant antibodies and equilibrium affinity data obtained with previously reported purified mutant monoclonal antibodies was observed. Approximately 75% of the single amino acid mutants exhibited significant binding to one or more of the digoxin analogs. Mutations that alter and, in some cases, reverse specificity for the different digoxin analogs were identified. *In vitro* scanning saturation mutagenesis represents a new tool for protein structure-function and engineering studies and can be interfaced with laboratory automation so that an even higher throughput of protein mutants can be constructed and analyzed.**

Structure-guided site-specific mutagenesis represents a powerful tool for the dissection and engineering of protein–ligand interactions (1, 2). One particularly useful mutagenesis technique is alanine scanning mutagenesis in which a number of residues are substituted individually with the amino acid alanine so that the effects of losing side-chain interactions can be determined, while minimizing the risk of large-scale perturbations in protein conformation (3). However, the substitution of functional residues with alanine or any other single amino acid can give misleading results regarding their mechanistic importance (4).

Tremendous attention continues to be focused on antibodies because they define a paradigm of high-affinity protein binding and they are among the most important classes of commercial protein molecules. Antigen binding is determined primarily, but not exclusively, by amino acid residues in the antibody hypervariable or complementarity determining regions I, II, and III of the heavy (H) and light (L) chains. Site-specific mutagenesis and the screening of antibody libraries by phage display have been used to explore the effect of amino acid substitutions on antigen affinity (5–13). Such studies have demonstrated that even antibodies generated from the secondary immune response are not necessarily "optimized" with respect to affinity and/or specificity (10–13). There is evidence that the antigen binding site exhibits a fair degree of plasticity in that a number of amino acid substitutions are tolerated and occasionally improve affinity (6, 12).

Comprehensive information on the functional significance and information content of a given residue of an antibody can best be obtained by saturation mutagenesis in which all 19 amino acid substitutions are examined. The shortcoming of this approach is that the logistics of multiresidue saturation mutagenesis are daunting (4, 14). Hundreds, and possibly even thousands, of site specific mutants must be studied. For each mutant protein, the appropriate gene construct must be made, the DNA must be transformed into a host organism, transformants need to be selected and screened for expression of the protein, the cells have to be grown to produce the protein, and finally the recombinant mutant protein must be isolated. There have been only a handful of studies where one, or at most a few, residues in an antibody have been subjected to saturation mutagenesis. Even in those studies, only some of the mutants were examined in detail (5, 6, 15).

In recent years, techniques for estimating the equilibrium constant for ligand binding using minuscule amounts of protein have been developed (16–18). In this work we have shown that the ability to perform functional assays with small amounts of material can be exploited to develop highly efficient, *in vitro* methodologies for the saturation mutagenesis of antibodies. We have bypassed all time-consuming cloning steps by combining PCR mutagenesis with coupled *in vitro* transcription/translation for the high throughput generation of protein mutants. Here, the PCR products are used directly as the template for the *in vitro* transcription/translation of the mutant single chain antibodies. Because of the high efficiency with which all 19 amino acid substitutions can be generated and analyzed in this way, it is now possible to perform saturation mutagenesis on numerous residues of interest, a process that can be described as *in vitro* scanning saturation mutagenesis.

A high-affinity anti-digoxin single chain Fv (scFv(Dig)) (19) derived from the well-studied anti-digoxin 26–10 murine monoclonal antibody (20) was selected as a model system for our studies. Digoxin and related cardiac glycosides consist of a 5β,14β-steroid body, linked to an α,β-unsaturated lactone at C17 and an O-linked carbohydrate at position 3. The 26–10 antibody binds to the cardiac glycosides digoxin, digitoxin, and digoxigenin with high-affinity ($K_a \approx 9 \times 10^9\ M^{-1}$) and with a 42-fold lower affinity to ouabain (21). The three-dimensional structure of the 26–10 Fab complexed with digoxin (22) reveals that the 3′-tridigitoxose is exposed to the solvent, whereas the lactone ring is fully buried at the bottom edge of the binding site (Fig. 1). Unlike other antibody–antigen complexes (23), binding does not appear to cause detectable conformational changes of either the antibody or the hapten. Both affinity and specificity are derived entirely from shape complementarity,

The publication costs of this article were defrayed in part by page charge payment. This article must therefore be hereby marked "*advertisement*" in accordance with 18 U.S.C. §1734 solely to indicate this fact.

0027-8424/97/94412-6$2.00/0
PNAS is available online at **http://www.pnas.org.**

Abbreviations: H, heavy; L, light.

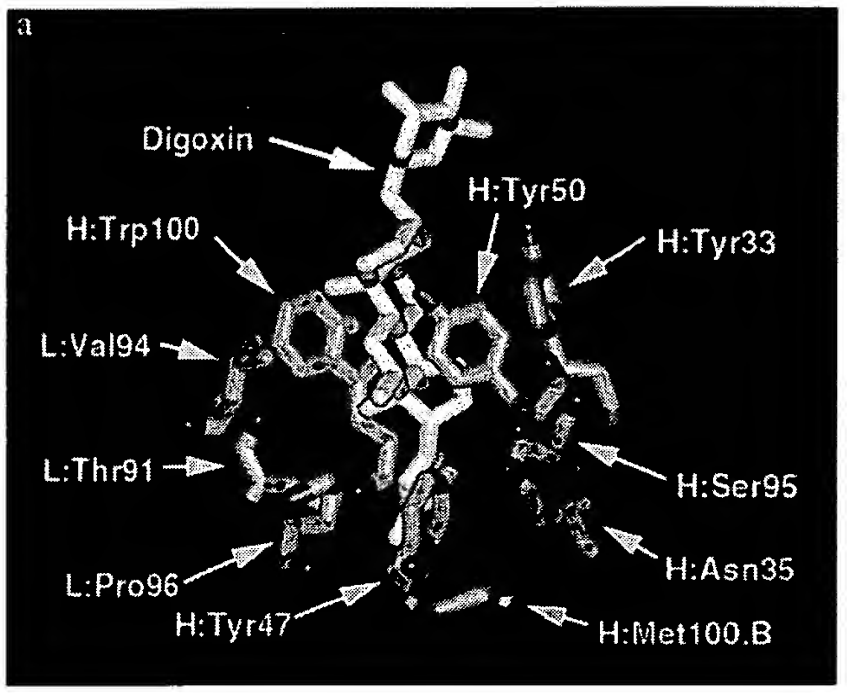

b

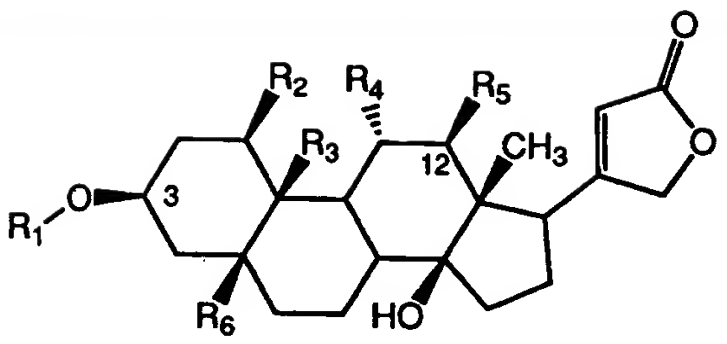

	R_1	R_2	R_3	R_4	R_5	R_6
Digoxin	Sugars	H	CH_3	H	OH	H
Digitoxin	Sugars	H	CH_3	H	H	H
Digoxigenin	H	H	CH_3	H	OH	H
Ouabain	Sugar	OH	CH_2OH	OH	H	OH

FIG. 1. (*a*) Computer model showing bound digoxin and 10 residues that define the 26–10 binding pocket. This figure was generated using Quanta CHARMM software (Micron Separations) using the coordinates of Jeffery *et al.* (22). (*b*) Structures of digoxin and the three analogs used in these studies.

since no hydrogen bonds have been identified between digoxin and the antibody.

In vitro scanning saturation mutagenesis was used to analyze the role and plasticity of six key contact residues in the scFv(Dig). The relative affinities of a total of 114 mutant antibodies for digoxin, digitoxin, digoxigenin, and ouabain were determined resulting in the generation of a comprehensive data base of 456 relative affinity values.

MATERIALS AND METHODS

Taq polymerase was purchased from Promega, dNTPs from Pharmacia, and oligonucleotide primers from Midland Certified Reagent (Midland, TX). Pyruvate kinase, tRNA, and nucleotide triphosphates were obtained from Boehringer Mannheim. Digoxin and digitoxin were purchased from Sigma.

PCR Mutagenesis. Mutations in the scFv(digoxin) antibody were generated by the overlapping PCR method (24–26). Briefly, the plasmid pET25b(scFv(Dig)) (27) was used as a template for PCR. For the first round PCR, a 2-kb *Nde*I–*Pvu*I fragment from pET25b(scFv(Dig)) was used as the 3′ template, whereas a 4-kb *Xho*I–*Pvu*I fragment was used as the 5′ template. The restriction fragments were isolated on an agarose gel to eliminate the possibility that any contaminating full-length, wild-type scFv(Dig) construct was present. A list of the primers used for the first and second PCR steps is available upon request from the authors. First round PCR was carried out in 50 mM KCl, 10 mM Tris·HCl (pH 9.0) at 25°C/0.1% Triton X-100, 0.2 mM dNTPs, 2.5 units *Taq* polymerase (Promega), 0.6 μM each of the two primers, and 0.05 μg template in 100 μl total volume. Amplification was carried out using the following sequence: one cycle at 94°C for 2 min; 29 cycles consisting of 94°C for 1 min, 55°C 2 min, and 72°C for 3 min; one cycle of 94°C for 1 min, 55°C for 2 min, and 72°C for 10 min. The PCR products from the first round were gel-purified and used, together with outside primers, in the overlap extension PCR reaction. For this round of PCR, the mix contained 50 mM KCl, 10 mM Tris·HCl (pH 9.0) at 25°C/0.1% Triton X-100, 0.2 mM dNTPs, 2.5 units *Taq* polymerase (Promega), 0.6 μM each of the two primers, and 0.05 μg each of both the 5′ template and the 3′ template in 100 μl total volume. The amplification sequence for the overlap extension reaction was the same as for the first round reactions except that the annealing temperature for the first five cycles was set between 48°C and 55°C, depending on the melting temperature of overlapping sequence. The PCR products were ethanol precipitated and the pellets were resuspended in 100 μl of water.

***In Vitro* Transcription/Translation.** *In vitro* protein synthesis using an *Escherichia coli* coupled transcription/translation system was carried out essentially as described (28). T7 RNA polymerase and S30 *E. coli* extract for coupled transcription/translation were prepared using standard procedures (28, 29). The coupled transcription/translation reactions were carried out in 30 μl total volume and the reaction mix contained the following: 55 mM Tris acetate (pH 7.8), 2 mM DTT, 1.2 mM ATP, 0.8 mM CTP, 0.8 mM GTP, 0.8 mM UTP, 2% polyethylene glycol (M_r, 8000), 27 mM phospho*enol*pyruvate, 0.4 mM cAMP, 35 μg/ml folinic acid, 30 mM ammonium acetate, 72 mM KOAc, 1.5 mM $Ca(OAc)_2$, 0.35 mM of each amino acid, 0.5 mM EDTA, 0.3 mM glucose 6-phosphate, 2 μg T7 RNA polymerase, 0.4 μg pyruvate kinase, 20 μg tRNA, 5 μg rifampicin, 13.3 mM $Mg(OAc)_2$, and 5 μl of *E. coli* S30 fraction. Reactions were initiated by adding 0.5 μg of the DNA produced by overlap extension in 7 μl. For radiolabeling of the protein synthesis products 0.083 mM of ^{35}S-methionine (1175 Ci/mmol, 1 Ci = 37 GBq; New England Nuclear), was added to the reaction mix. Reactions were incubated for 25 min at 37°C with gentle shaking and were stopped by placing on ice.

General Procedures. SDS/PAGE was carried out in 15% polyacrylamide gels (30). Overlap extension PCR products were sequenced by the dideoxy sequencing method. Representative PCR products were also sequenced following subcloning into pET25b(scFv(Dig)). The digoxin–BSA, digitoxin–BSA, and ouabain–BSA conjugates used in the ELISA analysis were prepared via oxidation of the terminal sugar residues with $NaIO_4$ followed by covalent attachment to BSA through reductive amination in the presence of $NaBH_4$ (31). The digoxigenin–BSA conjugate was prepared from a direct reaction between BSA and 3-aminodeoxydigoxigenin hemisuccinimide (Molecular Probes) according to the manufacturer's instructions.

ELISA. Antibody capture ELISA was performed using standard procedures (32), using 1% (wt/vol) boiled powdered milk (Carnation) as the blocking agent. The plates were washed three times and were developed with the colorimetric horseradish peroxidase substrate 2,2′-azine-bis(3-ethylbenzothiazoline)-6-sulfonic acid diammonium salt (ABTS) (Pierce). The absorbance of each well of the ELISA plates was measured at 405 nm on a microplate autoreader when the ABTS reaction was still in the linear range, a fact that was confirmed by taking several time points per plate. For each cardiac glycoside being investigated (digoxin, digitoxin, digoxigenin, ouabain) the absorbances for each mutant were linearly scaled to that of the wild-type scFv(Dig), which was assigned a value of 1.0, then plotted in the histograms of Fig. 2. Wild-type scFv(Dig) was

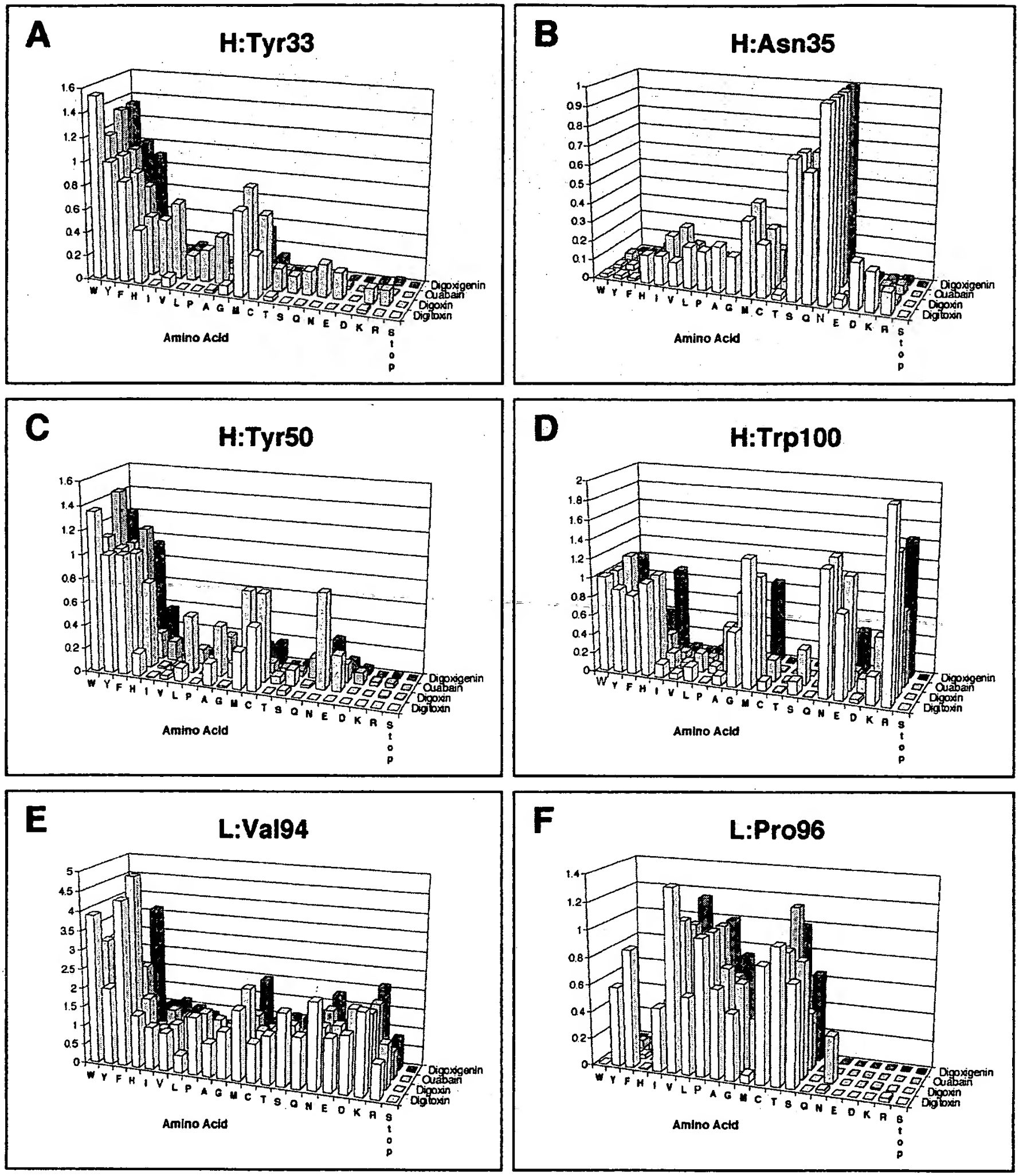

FIG. 2. Histograms of the ELISA data for the different mutant proteins binding to digoxin, digitoxin, digoxigenin, and ouabain. (*A*) Mutations of residue H:Tyr-33. (*B*) Mutations of residue H:Asn-35. (*C*) Mutations of residue H:Tyr-50. (*D*) Mutations of residue H:Trp-100. (*E*) Mutations of residue L:Val-94. (*F*) Mutations of residue L:Pro-96. The plotted values correspond to the absorbance observed in ELISA measured at 405 nm on a microplate autoreader when the ABTS reaction was still in the linear range, a fact that was confirmed by taking several time points per plate. For each cardiac glycoside being investigated (digoxin, digitoxin, digoxigenin, ouabain) the absorbances for each mutant were linearly scaled to that of the wild-type scFv(Dig), which was assigned a value of 1.0, then plotted in the histograms. Wild-type scFv(Dig) was included on every ELISA plate to provide an internal calibration of the data.

included on every ELISA plate to provide an internal calibration for results obtained on different plates. A comprehensive numerical table of the scaled ELISA data is available upon request from the authors.

RESULTS

Our initial *in vitro* scanning saturation mutagenesis studies were performed on six residues that help define the interior of the anti-digoxin 26–10 antibody binding pocket (22). The

single chain Fv form (scFv(Dig)) of the 26–10 antibody was used (19, 27, 33), since the presence of only one polypeptide chain eliminates chain association difficulties that are possible with Fab antibodies. The six chosen 26–10 residues consisted of three aromatic residues that define the largely hydrophobic walls of the binding pocket and thereby make extensive Van der Waals contact with hapten (heavy chain residues H:Tyr-33, H:Tyr-50, and H:Trp-100), a residue that forms hydrogen bonds with contact residues and therefore is presumably of importance in maintaining the architecture of the binding pocket (H:Asn-35) and, finally, two residues that define the bottom of the binding pocket (light chain residues L:Val-94 and L:Pro-96).

For each chosen residue, 21 genes encoding all possible amino acid substitutions, as well as a double stop codon (control), were constructed by overlap extension PCR. All amino acid substitutions were encoded by *E. coli* preferred codons. To eliminate the possibility of contamination with wild-type template, the 3′ and 5′ fragments in the first round PCR were amplified from the respective gel purified restriction fragments as described in *Materials and Methods*. The final products of the overlap extension PCR reaction contain a T7 promoter and ribosome binding site in front of the scFv(Dig) gene. A herpes simplex virus sequence is also present at the end of the scFv(Dig) gene, so that the scFv(Dig) protein can be detected by ELISA using an anti-herpes simplex virus sequence monoclonal antibody.

The PCR overlap extension products were used as templates for coupled *in vitro* transcription/translation reactions to produce functional scFv(Dig) proteins. The same amount of template was used for each coupled *in vitro* transcription/translation reaction. An *E. coli* S30 ribosomal extract, as opposed to mammalian or plant cell extracts, was used for *in vitro* translation because the bacterial system has the significant advantage of eliminating the need to cap the message. The reactions were run on a 30 μl scale for 25 min at 37°C. Preliminary experiments established that the reaction is completed after 25 min (29). SDS/PAGE autoradiography, Western blots, and hot trichloroacetic acid precipitation of the translation products labeled with [^{35}S]methionine all demonstrated that similar concentrations of polypeptide, ≈10 nM judging from ELISA comparison to an authentic sample of wild-type scFv, are produced in the different transcription/translation reactions using the above protocol, irrespective of the amino acid substitution (29).

The protein products from the coupled *in vitro* transcription/translation step were analyzed by ELISA. Briefly, 96-well microtiter plates were coated with the BSA conjugate of digoxin, digitoxin, digoxigenin, or ouabain. The microtiter plates were then incubated with equal amounts from each of the *in vitro* synthesis reactions. To provide accurate calibration, the construct prepared with the wild-type sequence was used on each ELISA plate. It should be noted that the wild-type construct was produced by the overlapping PCR method alongside the mutants, thereby providing an accurate calibration for all stages of the procedure.

Because of the large number of samples involved in the *in vitro* saturation mutagenesis experiments, several "quality control" tests were conducted at key points. Specifically: (*i*) A gel of the PCR products was run prior to the coupled *in vitro* transcription/translation reactions. This analysis confirmed that the correct size products had been produced and also enabled determination of the amount of amplified DNA template to be used in the *in vitro* protein synthesis step. (*ii*) [^{35}S]Methionine was added to the translation mixture and the protein products were analyzed by SDS/PAGE and autoradiography. Western blots were also used to analyze the protein products, using an anti-herpes simplex virus monoclonal antibody for detection. Protein products of the appropriate length and in similar quantities were observed for the different reactions. (*iii*) As mentioned previously, a control reaction that places two adjacent stop codons at the position being mutagenized was carried out every time. Two adjacent stop codons were used to eliminate possible readthrough. Autoradiography of the *in vitro* protein synthesis products confirmed that only truncated polypeptides of the anticipated molecular weight were detected in these control reactions. The truncated scFv(Dig) polypeptides generated by stop codon insertion exhibit no hapten binding and were thus used to establish the baseline in the ELISA assays. (*iv*) For each residue, the entire process was carried out in at least two independent runs to verify the reproducibility of the results. In addition, each ELISA was run in duplicate. Using the protocols described, the reproducibility of the data was excellent with absorbance values >20% of wild-type, varying by no more than ±5% between experiments (performed by different investigators). ELISA values lower than 20% of wild type exhibited a greater degree of variability, presumably because of the lower signal-to-noise ratio. A low or absent ELISA signal means that the off-rate is too fast for the scFv(Dig) mutants to remain bound to a significant extent during the incubations and washing steps, but does not necessarily imply complete loss of binding.

The ELISA results for the different mutants binding to digoxin and the three analogs (456 relative affinity values in all) are plotted as histograms in Fig. 2. All absorbance values are normalized to the wild-type construct to allow for direct comparisons. Schildbach *et al.* (21) have reported that the relative digoxin:digitoxin, digoxin:digoxigenin, and digoxin :ouabain affinities are 2:1, 1:1, and 42:1, respectively. Therefore, the relative ELISA values for the different cardiac glycosides in Fig. 2*A–F* must be scaled accordingly before any direct comparisons are made.

DISCUSSION

A striking feature of the data shown in Fig. 2 is that 86 of the 114 substitutions in residues H:Tyr-33, H:Asn-35, H:Tyr-50, H:Trp-100, L:Val-94, or L:Pro-96 result in significant (>15% of wild-type) recognition and binding to one or more of the digoxin analogs. The large number of amino acid substitutions that can be tolerated is highly indicative of the plasticity of the antigen binding site. Other studies have also indicated that single amino acid mutations in the complementarity determining regions generally do not abolish binding to haptens (6, 7). Chen and colleagues have suggested that the ability of antibody genes to tolerate single amino acid mutations is of significance for somatic hypermutation because it allows mutated B lymphocytes to remain functional while undergoing further affinity maturation (6).

None of the amino acid replacements of L:Val-94 abolishes antigen binding. This result is probably related to the fact that in the crystal structure the side chain of L:Val-94 does not directly contact digoxin (22). Several substitutions at L:94 gave a higher absorbance reading in the ELISA assays compared with wild-type valine. A higher ELISA signal can result either from improved binding affinity, more efficient folding, or avidity effects due to dimerization. The latter is not likely in this case because the scFv(Dig) concentrations produced by *in vitro* translation are low, making dimerization highly unfavorable. It is not possible to distinguish from the ELISA alone between mutants that fold more efficiently and those having a higher affinity for the hapten. Nevertheless, it is noteworthy that in the case of L:Val-94 mutants, the highest absorbance values (Fig. 2*E*) were observed with aromatic amino acid substitutions that should result in a larger hapten contact area. Hydrophobic substitutions such as L:Val-94-Phe, L:Val-94-Trp, or L:Val-94-Tyr could presumably improve digoxin binding relative to the wild-type scFv(Dig) antibody by making additional Van der Waals contacts. Regardless of the detailed explanation, our results emphasize that not all residues are

optimized in even high-affinity antibodies such as 26–10, and that the absence of close contact with the hapten confers higher plasticity, i.e., the ability to tolerate a wider range of substitutions without compromising binding.

High-affinity scFv(Dig) mutants selected by fluorescence-activated cell sorting from a library displayed on the surface of *E. coli* (33) had predominantly aromatic substitutions at L:Val-94 (P. Daugherty, G.C., B.L.I., and G.G., unpublished work). The high representation of aromatic residues in clones selected from a library is consistent with the increased hapten binding data of the respective *in vitro* synthesized clones.

For the three heavy chain aromatic residues that make substantial Van der Waals contacts with bound digoxin, H:Tyr-33, H:Tyr-50, and H:Trp-100, conservative changes to any of the other aromatic amino acids largely retained or slightly improved the ELISA signal and there was little effect on specificity. The smaller, more polar histidine was tolerated noticeably less well than the other aromatic amino acids, supporting the notion that hydrophobic contact surface area is important in these positions. Methionine retained substantial activity in all three cases, a fact that is consistent with a ranking of this amino acid close to the large aromatic amino acids in both size and hydrophobicity indices (34). However, it is important to note that large aromatic amino acids are not essential for binding at any one of the positions (H:33, H:50, or H:100). Substitution of Asn for H:Tyr-50 or H:Trp-100 had only a slight effect on digoxin binding, but diminished activity was observed when substituted for H:Tyr-33. Somewhat surprisingly, the positively charged residues lysine and arginine retained partial and full digoxin binding activity, respectively, when substituted for H:Trp-100. It is noteworthy that the highest affinity mutant isolated from a heavy chain library in which H:Trp-100 was mutagenized also had an arginine at H:100 (P. Daugherty, unpublished work).

Our results with H:Asn-35 are consistent with this residue playing largely a structural role in the scFv(Dig) binding pocket owing to specific hydrogen bonds to H:Tyr-47, as well as the H:Ser-95 that were identified in the crystal structure of 26–10 (22). The most active replacements for H:Asn-35, namely H:Asn-35Gln and H:Asn^{35}Ser, have side chains that also can potentially take part in hydrogen bonding.

In general, digoxigenin binding correlated with digoxin binding, a fact that is consistent with the minimal role that the sugar moieties appear to play in the binding of digoxin by the 26–10 antibody (22). Moreover, out of the 114 mutants examined, none displayed significantly enhanced affinity for ouabain relative to the other derivatives. Ouabain is larger than the other cardiac glycosides examined and is not accommodated as well in the binding pocket of 26–10 as evidenced by the lower affinity (21). Therefore, an increase in ouabain specificity relative to digoxin should require extensive alterations of the binding site that are not feasible within the context of single amino acid substitutions. On the other hand, a significant change in specificity for digitoxin versus digoxin was observed with certain mutants. For example, L:Pro-96-Tyr or especially L:Pro-96-Phe mutants exhibit binding to digitoxin comparable to wild-type scFv(Dig), whereas binding to digoxin was substantially diminished. The crystal structure (22) indicates that L:Pro-96 is adjacent to the C12 hydroxyl of digoxin, which is absent in digitoxin (Fig. 1). Computer modeling suggests that side chains having smaller volume are capable of accommodating both digoxin and digitoxin. However, digoxin binding is sterically hindered by the larger side chains of L:Pro-96-Phe or L:Pro-96-Tyr, whereas digitoxin binding is not. In agreement with this explanation, the other two molecules with hydroxyl groups at C12, namely ouabain and digoxigenin, also exhibit no binding with the L:Pro-96-Phe and L:Pro-96-Tyr mutants. In the case of L:Pro-96-Trp it appears that the indole ring of tryptophan abolishes binding to any of the haptens either because it causes a large perturbation in the binding pocket or it is simply too large to accommodate even the C12 hydrogen of digitoxin.

Mutants are also observed that retain high affinity for digoxin, while exhibiting substantially decreased binding to digitoxin. Noteworthy examples include several mutants of H:Tyr-33, such as H:Tyr-33-Ile or H:Tyr-33-Asn, and especially H:Tyr-50-Asn. It is unclear from the crystal structure why these residues, which are far from the C12 position of bound digoxin, have such a strong influence on the specificity of digoxin versus digitoxin binding.

There is excellent agreement between the values for relative affinities and specificities for the different digoxin mutants in the literature (12, 21, 35, 36) and the data in Fig. 2. For example, Schildbach *et al.* (21) prepared and analyzed several H:Tyr-50 mutants of the 26–10 IgG. The relative order of digoxin affinities measured by Schildbach *et al.* listed from highest to lowest affinity, for the different H:Tyr-50 mutants was as follows: H:Tyr-50 (wild type) ~ H:Tyr-50-Trp ~ H:Tyr-50-Phe > H:Tyr-50-Asn > H:Tyr-50-His > H:Tyr-50-Leu > H:Tyr-50-Ala > H:Tyr-50-Gly and H:Tyr-50-Asp (34). The H:Tyr-50-Asn and H:Tyr-50-Asp mutants were reported to have increased specificity in favor of digoxin over digitoxin binding. Similarly, Near *et al.* (36) produced and measured the relative affinities for certain H:Asn-35 mutants. The reported order of affinities are H:Asn-35 (wild type) > H:Asn-35-Gln > H:Asn-35-Val > H:Asn-35-Thr > H:Asn-35-Leu > H:Asn-35-Ala and H:Asn-35-Asp (36). Comparison of these data with Fig. 2 reveals good agreement with our ELISA results. Such agreement indicates that the folding efficiencies for the different scFv(Dig) mutants in our experiments, at least those mentioned above, must be comparable so that the ELISA signals reflect primarily the relative affinities of the different mutants. Moreover, it underscores the validity of our methodology for the rapid generation and characterization of mutant antibodies. Finally, comparison of the literature values for the lower affinity mutants and our ELISA measurements place an approximate limit of between 10^6 and 10^7 M^{-1} for the lowest affinity observable in our ELISAs.

It is possible that as *in vitro* scanning saturation mutagenesis is applied to other proteins, or even perhaps other residues of scFv(Dig), there will be instances where certain mutations may affect the concentration of correctly folded protein obtained by *in vitro* transcription/translation, thereby prohibiting the interpretation of the ELISA results solely on the basis of antigen affinity. Even in the case when an ELISA signal does not indicate a difference in affinity, ELISA readings substantially higher than wild-type are of interest since they identify residues that facilitate higher levels of expression or correct folding, critical issues in the large scale expression of scFv antibodies for practical purposes.

As we have demonstrated in this report, *in vitro* scanning saturation mutagenesis provides a rapid method for obtaining a large amount of structure-function information including: (*i*) identification of residues that modulate ligand binding specificity, (*ii*) a better understanding of ligand binding based on the identification of those amino acids that retain activity and those that abolish activity at a given location, (*iii*) an evaluation of the overall plasticity of an active site or protein subdomain, (*iv*) identification of amino acid substitutions that result in increased binding.

The *in vitro* saturation mutagenesis of one residue can be completed in duplicate within a week by a single investigator. In addition, several of the steps are amenable to robotic automation, which could increase the throughput of mutants studied even further. *In vitro* scanning saturation mutagenesis should prove particularly valuable for protein engineering studies, even with enzymes when coupled to a catalytic assay, as a rapid way of identifying mutants with interesting properties that can then be produced in bacteria and subjected to more detailed structural and functional characterization. In

addition, *in vitro* scanning saturation mutagenesis represents a systematic new tool for exploring *in vitro* antibody affinity evolution, analogous to somatic hypermutation *in vivo*. In particular, interesting single mutants could be used as a starting point for subsequent rounds of saturation mutagenesis, so that multiple mutations with additive effects on binding could be identified. This same sequential mutation approach should be useful with other types of proteins, so that attributes such as expression level, folding ability, catalytic rate or substrate specificity could be modulated in a systematic way.

We are grateful to Patrick Daugherty and Dr. Boyd Hardesty for reading the manuscript. This work was supported by Grant NSF BES 94-2502 to B.L.I. and G.G.

1. Wells, J. A. (1996) *Proc. Natl. Acad. Sci. USA* **93,** 1–6.
2. Braisted, A. C. & Wells, J. A. (1996) *Proc. Natl. Acad. Sci. USA* **93,** 5688–5692.
3. Cunningham, B. C., Jhurani, P., Ng, P. & Wells, J. A. (1989) *Science* **243,** 1330–1336.
4. Warren, M. S., Marolewski, A. E. & Benkovic, S. J. (1996) *Biochemistry* **35,** 8855–8862.
5. Ito, W., Iba, Y. & Kurosawa, Y. (1993) *J. Biol. Chem.* **268,** 16639–16647.
6. Chen, C., Robert, V. A., Stevens, S., Brown, M., Stenzel-Poore, M. P. & Rittenberg, M. B. (1995) *EMBO J.* **14,** 2784–2794.
7. Brown, M., Rittenberg, M. B., Chen, C. & Roberts, V. A. (1996) *J. Immunol.* **156,** 3285–3291.
8. Harrison, J. L., Williams, S. C., Winter, G. & Nissim, A. (1996) *Methods Enzymol.* **267,** 109–115.
9. Burton, D. R. & Barbas, C. F., III (1994) *Adv. Immunol.* **57,** 191–280.
10. Yelton, D. E., Rosk, M. J., Cruz, G., Cosand, W. L., Bajorath, J., Hellstrom, I., Hellstrom, K. E., Huse, W. D. & Glaser, S. M. (1995) *J. Immunol.* **155,** 1994–2004.
11. Jackson, J. R., Sathe, G., Rosenberg, M. & Sweet, R. (1995) *J. Immunol.* **154,** 3310–3319.
12. Short, M. K., Jeffery, P. D., Kwong, R.-F. & Margolies, M. N. (1995) *J. Biol. Chem.* **270,** 28541–28550.
13. Wong, Y. W., Kussie, P. H., Parhami-Seren, B. & Margolies, M. N. (1995) *J. Immunol.* **154,** 3351–3358.
14. Hilton, D. J., Watowich, S. S., Katz, L. & Lodish, H. F. (1996) *J. Biol. Chem.* **271,** 4699–4708.
15. Brummell, D. A., Sharma, V. P., Anand, N. N., Bilous, D., Dubuc, G., *et al.* (1993) *Biochemistry* **32,** 1180–1187.
16. Parker, C. W. (1978) in *Handbook of Experimental Immunology,* ed. Weir, D. M. (Blackwell Scientific, Oxford), 3rd Ed.
17. Blackburn, G. F., Shah, H. P., Kenten, J. H., Leland, J., Kamin, R. A., Link, J., Peterman, J., Powell, M. J., Shah, A., Talley, D. B., Tyagi, S. K., Wilkins, E., Wu, T. G. & Massey, R. J. (1991) *Clin. Chem.* **37,** 1534–1539.
18. Bard, A. J. & Whitsides, G. (1993) U.S. Patents 5,221,605 and 5,238,808.
19. Huston, J. S., Levinson, D., Mudgett-Hunter, M., Tai, M.-S., Novotny, J. S., Margolies, M. N., Ridge, R. J., Bruccoleri, R. E., Haber, E., Crea, R. & Opperman, H. (1988) *Proc. Natl. Acad. Sci. USA* **85,** 5879–5883.
20. Mudgett-Hunter, M., Margolies, M. N., Ju, A. & Haber, E. (1982) *J. Immunol.* **129,** 1165–1172.
21. Schildbach, J. F., Near, R. I., Bruccoleri, R. E., Haber, E., Jeffery, P. D., Ng, S.-C., Novotny, J., Sheriff, S. & Margolies, M. N. (1993) *J. Biol. Chem.* **268,** 21739–21747.
22. Jeffery, P. D., Strong, R. K., Sieker, L. C., Chang, C. Y. Y., Campbell, R. L., Petsko, G. A., Haber, E., Margolies, M. N. & Sheriff, S. (1993) *Proc. Natl. Acad. Sci. USA* **90,** 10310–10314.
23. Braden, B. C. & Poljak, R. J. (1995) *FASEB J.* **9,** 9–16.
24. Ho, S. N., Hunt, H. D., Horton, R. M., Pullen, J. K. & Pease, L. R. (1989) *Gene* **77,** 51–59.
25. Horton, R. M. & Pease, L. R. (1991) in *Directed Mutagenesis: A Practical Approach,* ed. McPherson, M. J. (Oxford Univ. Press, New York), pp. 217–247.
26. Higuchi, R., Krummel, B. & Saiki, R. K. (1988) *Nucleic Acids Res.* **16,** 7351–7367.
27. Burks, E. A. & Iverson, B. L. (1995) *Biotechnol. Prog.* **11,** 112–114.
28. Kudlicki, W., Odom, O. W., Kramer, G. & Hardesty, B. (1994) *J. Biol. Chem.* **269,** 16549–16553.
29. Burks, E. A. (1996) Ph.D. thesis (University of Texas, Austin).
30. Laemmli, U. K. (1970) *Nature (London)* **227,** 680–685.
31. Smith, T. W., Bulter, V. P., Jr., & Haber, E. (1970) *Biochemistry* **9,** 331–337.
32. Harlow, E. & Lane, D. (1988) *Antibodies: A Laboratory Manual* (Cold Spring Harbor Lab. Press, Plainview, NY).
33. Francisco, J. A., Campbell, R., Iverson, B. L. & Georgiou, G. (1993) *Proc. Natl. Acad. Sci. USA* **90,** 10444–10448.
34. Tomii, K. & Kanehisa, M. (1996) *Protein Eng.* **9,** 27–36.
35. Schildbach, J. F., Shaw, S.-Y., Bruccoleri, R. E., Haber, E., Herzenberg, L. A., Jager, G. C., Jeffery, P. D., Panka, D. J., Parks, D. R., Near, R. I., Novotny, J., Sheriff, S. & Margolies, M. N. (1994) *Protein Sci.* **3,** 737–749.
36. Near, R. I., Mudgett-Hunter, M., Novotny, J., Bruccoleri, R. & Ng, S. C. (1993) *Mol. Immunol.* **30,** 369–377.

Amino acids are the basic structural units of proteins. An amino acid consists of an amino group, a carboxyl group, a hydrogen atom, and a distinctive R group bonded to a carbon atom, which is called the α-carbon (Figure 2-5). An R group is referred to as a *side*

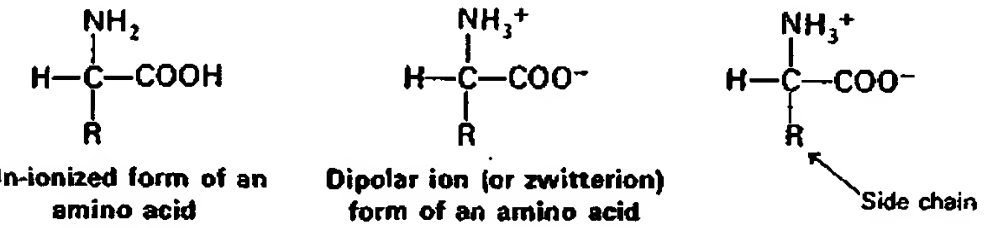

Figure 2-5
Structure of the un-ionized and zwitterion forms of an amino acid.

chain for reasons that will be evident shortly. Amino acids in solution at neutral pH are predominantly *dipolar ions* (or *zwitterions*) rather than un-ionized molecules. In the dipolar form of an amino acid, the amino group is protonated ($-NH_3^+$) and the carboxyl group is dissociated ($-COO^-$). The ionization state of an amino acid varies with pH (Figure 2-6). In acid solution (e.g., pH 1), the

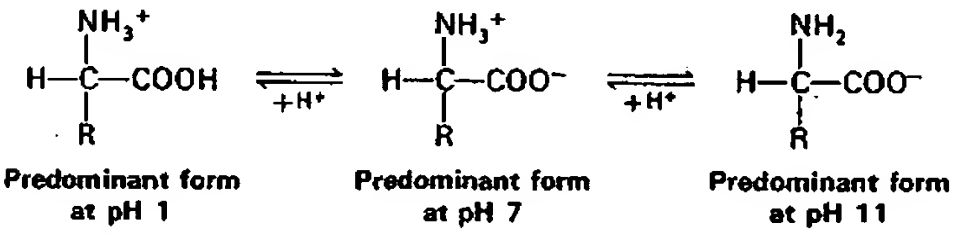

Figure 2-6
Ionization states of an amino acid as a function of pH.

carboxyl group is un-ionized ($-COOH$) and the amino group is ionized ($-NH_3^+$). In alkaline solution (e.g., pH 11), the carboxyl group is ionized ($-COO^-$) and the amino group is un-ionized ($-NH_2$). The concept of pH and the acid-base properties of amino acids are discussed further in the Appendix to this chapter.

The tetrahedral array of four different groups about the α-carbon atom confers optical activity on amino acids. The two mirror-image forms are called the L-isomer and the D-isomer (Figure 2-7). *Only L-amino acids are constituents of proteins.* Hence, the designation of the optical isomer will be omitted and the L-isomer implied in discussions of proteins herein, unless otherwise noted.

Twenty kinds of side chains varying in *size, shape, charge, hydrogen-bonding capacity, and chemical reactivity* are commonly found in proteins. Indeed, all proteins in all species, from bacteria to humans, are constructed from the same set of twenty amino acids. This fun-

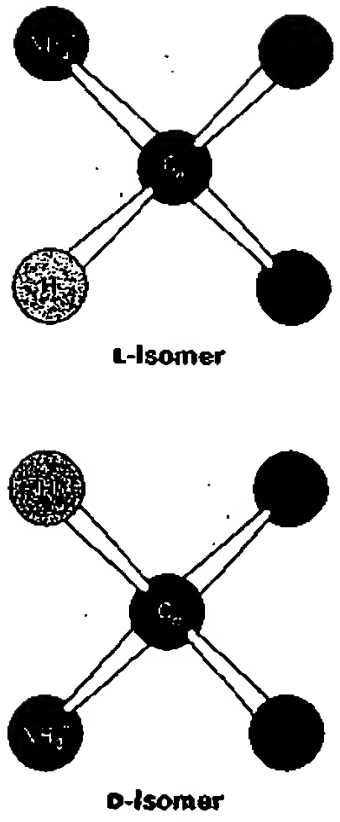

Figure 2-7
Absolute configurations of the L- and D-isomers of amino acids.

The side chains of the amino acids mentioned so far are uncharged at physiological pH. We turn now to some charged side chains. Lysine and arginine are positively charged at neutral pH, whereas whether histidine is positively charged or neutral depends on its local environment. These basic amino acids are shown in Figure 2-12. The negatively charged side chains are those of glu-

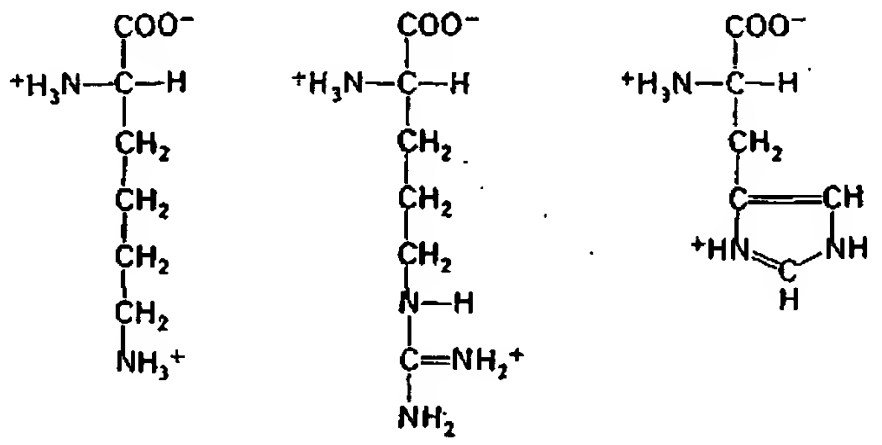

Figure 2-12
Lysine, arginine, and histidine have basic side chains.

tamic acid and aspartic acid (Figure 2-13). These amino acids will be called glutamate and aspartate to emphasize the fact that they are negatively charged at physiological pH. The uncharged derivatives of glutamate and aspartate are glutamine and asparagine (Figure 2-14), each of which contains a terminal amide group rather than a carboxylate. Finally, there are two amino acids whose side chains contain a sulfur atom: methionine and cysteine (Figure 2-15). As will be discussed shortly, cysteine plays a special role in some proteins by forming disulfide cross-links.

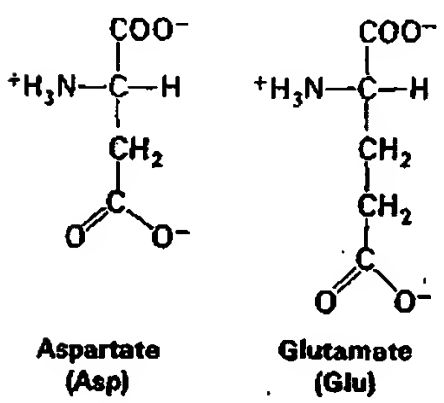

Figure 2-13
Aspartate and glutamate have acidic side chains.

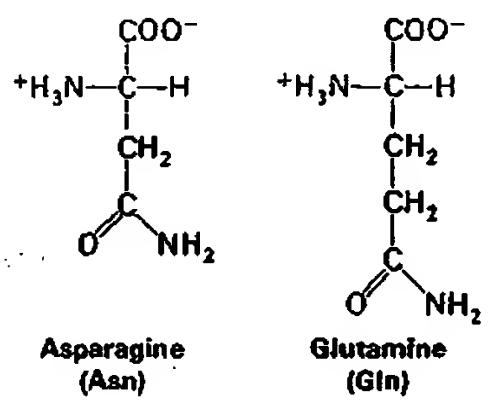

Figure 2-14
Asparagine and glutamine have amide side chains.

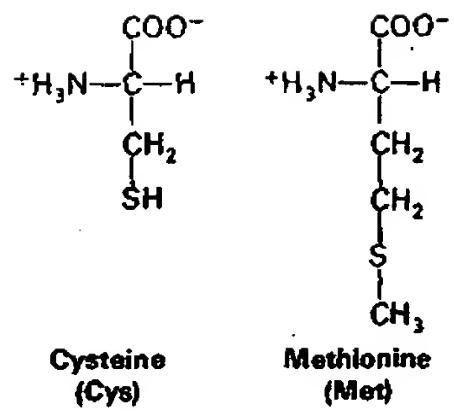

Figure 2-15
Cysteine and methionine have sulfur-containing side chains.

damental alphabet of proteins is at least two billion years old. The remarkable range of functions mediated by proteins results from the diversity and versatility of these twenty kinds of building blocks. In subsequent chapters, we will explore ways in which this alphabet is used to create the intricate three-dimensional structures that enable proteins to participate in so many biological processes.

Let us look at this repertoire of amino acids. The simplest one is glycine, which contains a hydrogen atom as its side chain (Figure 2-8). Alanine has a methyl group as its side chain. The other amino

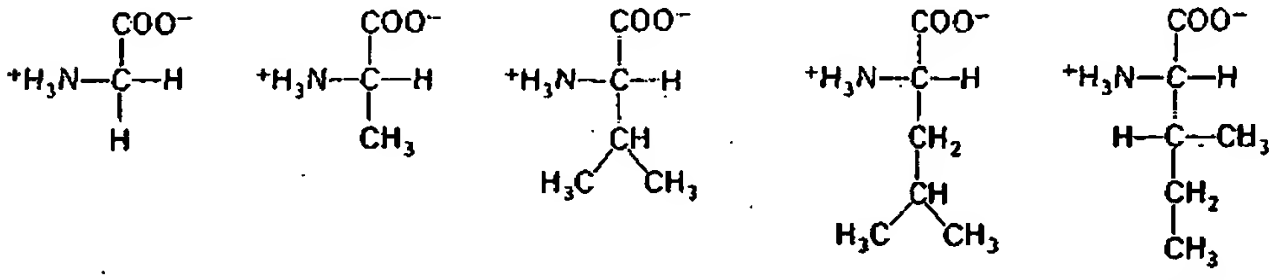

Figure 2-8
Amino acids having aliphatic side chains.

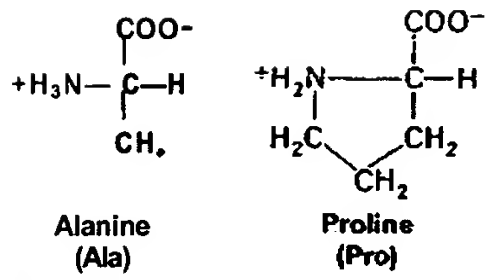

Figure 2-9
Proline differs from the other common amino acids in that it has a secondary amino group.

acids that have hydrocarbon side chains are valine, leucine, isoleucine, and proline. However, proline differs from the other amino acids in the basic set of twenty in that it contains a secondary rather than a primary amino group (Figure 2-9). Strictly speaking, proline is an imino acid rather than an amino acid. The side chain of proline is bonded to both the amino group and the α-carbon, which results in a cyclic structure.

Two amino acids, serine and threonine, contain aliphatic hydroxyl groups (Figure 2-10).

There are three common aromatic amino acids: phenylalanine, tyrosine, and tryptophan (Figure 2-11).

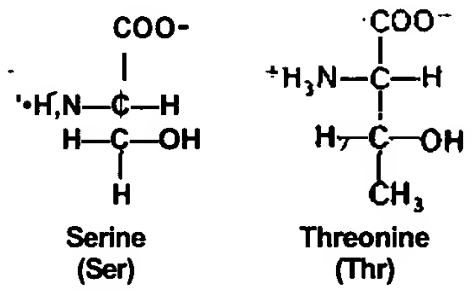

Figure 2-10
Serine and threonine have aliphatic hydroxyl side chains.

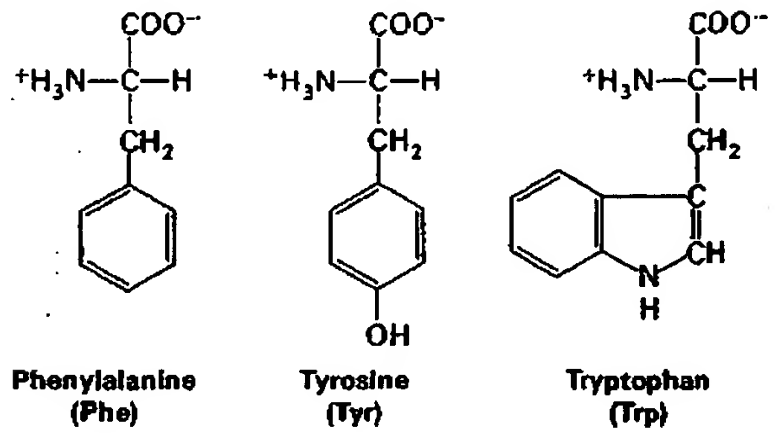

Figure 2-11
Phenylalanine, tyrosine, and tryptophan have aromatic side chains.